Progress in Nuclear Energy 187 (2025) 105825

Contents lists available at ScienceDirect

Progress in Nuclear Energy

journal homepage: www.elsevier.com/locate/pnucene

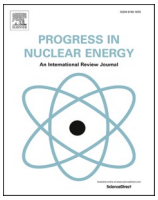

Safety margins improvement by means of the passive heat removal system and the HA-2 in VVER-1000/V320 reactors

Elena Redondo-Valero [a], Cesar Queral [b,*], Kevin Fernandez-Cosials [b], Victor Hugo Sanchez-Espinoza [c]

[a] NFQ Advisory Group, O'Donnell 34, 28009, Madrid, Spain
[b] Universidad Politécnica de Madrid (UPM), Ramiro de Maeztu 7, 28040, Madrid, Spain
[c] Karlsruhe Institute of Technology (KIT), Hermann-von-Helmholtz-Platz 1, Eggenstein-Leopoldshafen, 76344, Germany

ARTICLE INFO

Keywords:
Gen III/Gen III+ VVER
Passive heat removal system (PHRS)
SBO
Small and large break loss of coolant accidents (SBLOCA
LBLOCA)

ABSTRACT

One of the key functions of the safety systems is the removal of decay heat during an accidental sequence. Conventional VVER reactor designs have safety systems capable of removing residual heat in an emergency scenario, but these systems will be challenged to operate under station blackout conditions. As a result, some of the Gen III/Gen III + VVER designs incorporate passive safety systems capable of maintaining the decay heat removal in the event of a total loss of AC power. The present study focuses on the analysis of the air-cooled Passive Heat Removal System (PHRS) incorporated in some Gen III/Gen III + designs such as the VVER-1000/V412, the VVER-1200/V392M, V509, V523 or the VVER-TOI. For this purpose, a PHRS model has been developed in the TRACE system code, which has been incorporated into a model of a VVER-1000/V320 reactor which also includes another Gen III/Gen III + VVER reactors common feature; the Second Stage Hydro-accumulators (HA-2), subsystem of the Emergency Core Cooling System. Subsequently, a Station Blackout (SBO), a SBO along with an SBLOCA and a SBO along with an LBLOCA sequences have been analyzed with the air-cooled PHRS operating. The results show that in some scenarios, the PHRS performance is critical to lead the sequence to a safe state by transporting the decay heat to the atmosphere heat sink for at least 24 h.

Acronyms

Auxiliary Feed Water (AFW)	High Pressure Injection System (HPIS)
Steam Dump Valves to the Containment (BRU-A)	Heat Exchanger (HX)
Steam Dump Valves to the Condenser (BRU-K)	International Atomic Energy Agency (IAEA)
Steam Dump Valves to the Atmosphere (BRU-SN)	Isolation Condenser (IC)
Boiling Water Reactor (BWR)	Integrated Safety Analysis of Modular and Evolutive Reactors" (ISASMORE)
Core Damage (CD)	Karlsruhe Institute of Technology (KIT)
Cold Leg (CL)	Large Break Loss of Coolant Accident (LBLOCA)
Downcomer (DC)	Loss Of Offsite Power (LOOP)
Double Ended Guillotine Break (DEGB)	Low Pressure Injection System (LPIS)
Emergency Boron Injection System (EBIS)	Light Water Reactor (LWR)
Emergency Core Cooling System (ECCS)	Medium Break Loss of Coolant Accident (MBLOCA)
Emergency Diesel Generators (EDG)	Main Feed Water (MFW)
Emergency Feed Water (EFW)	Main Steam Isolation Valve (MSIV)
Event Tree (ET)	Nuclear Power Plant (NPP)
Generic Transient (GT)	Peak Cladding Temperature (PCT)
First Stage Hydroaccumulator (HA-1)	Passive Heat Removal System (PHRS)
Second Stage Hydroaccumulator (HA-2)	Pressurizer (PZR)
Hot Leg (HL)	Probabilistic Safety Analysis (PSA)
	Passive Safety System (PSS)

(continued on next column)

(continued)

(continued on next page)

* Corresponding author.
E-mail address: cesar.queral@upm.es (C. Queral).

https://doi.org/10.1016/j.pnucene.2025.105825
Received 2 August 2024; Received in revised form 25 March 2025; Accepted 30 April 2025
Available online 13 May 2025

Table 1
Passive Safety Systems classified by safety *functions* (Bryk et al., 2019; Buchholz et al., 2015; Heung Chang et al., 2013; IAEA, 2019, 2016; Kaliatka, 2017).

Emergency Core Cooling Systems	Accumulators	
	Make-up Tanks	
	Elevated Gravity Drain Tanks (inside/outside containment)	
	Recirculation valves or direct vessel injection connected to a RPV cavity	
Passive Heat Removal Systems	Through the SGs	Cooled by a water pool
		Cooled by air flow
	Through the RCS	Cooled by a water pool
		Cooled by a closed loop, having one HX inside the RPV and one HX in a water pool
Containment Cooling and Control Pressure	Suppression Pool	
	Containment Condenser (cooled by water or air)	
	Condensation on Containment inner wall	

(*continued*)

Pressure Water Reactor (PWR)
Reactor Coolant Pump (RCP)
Reactor Coolant System (RCS)
Reactor Pressure Vessel (RPV)
Small Break Loss of Coolant Accident (SBLOCA)
Station Blackout (SBO)
Success Criteria (SC)
Steam Generator (SG)
Thermal-Hydraulic (TH)
Turbine Trip (TT)
Steam Line (SL)
Small Modular Reactor (SMR)
Sodium Fast Reactors (SFR)

1. Introduction

According to the International Atomic Energy Agency (IAEA), Passive Safety Systems (PSS) are defined as "a System which is composed entirely of passive components and structures or a System which uses active components in a very limited way to initiate subsequent passive operation", (IAEA, 1994, 1991). Depending on the safety function they fulfil, the PSSs can be divided into three groups: Emergency Core Cooling Systems (ECCS), Passive Heat Removal Systems (PHRS) and Containment Cooling and Control Pressure, see Table 1 and (Bryk et al., 2019; Buchholz et al., 2015; Heung Chang et al., 2013; IAEA, 2019, 2016; Kaliatka, 2017).

The previous experience of the Universidad Politécnica de Madrid (UPM) with system codes such as TRACE regarding the PSSs is related to the following reactor designs and experimental facilities.

- MOTEL facility (natural circulation, helical-coil Steam Generators (SG), H2020 McSafer project) (Martinez-Gonzalez et al., 2024; Sanchez-Espinoza et al., 2021),
- ACME facility (PHRS, CMT, ACC, IRWST), which is part of the NEA ISP-51 project,
- Sirio facility (PHRS, H2020 PIACE Project) (De Grandis et al., 2019),
- Plant model: NuScale (1D, 3D models, ECCS and PHRS, H2020 McSafer project) (Redondo-Valero et al., 2022),
- Plant model: AP1000 (full plant model, PHRS, CMT, ACC, IRWST, PCS) (Queral et al., 2015, 2017),
- Plant model: VVER-1000 and VVER-1200 (air-cooled PHRS and HA-2),
- Plant model: CAREM-like (PHRS, 1D and 3D models),

The PHRS is a key factor of many Generation III/III + reactors, but it is not present in Generation II reactors, and therefore, the purpose of this paper is to present a detailed discussion of the safety margin provided by an air-cooled PHRS and the Second Stage Hydroaccumulators (HA-2) in a full plant model of a VVER-1000/V320 reactor. The HA-2 component is already described and analyzed extensively in (Elena Redondo-Valero et al., 2023), so in the present study the air-cooled PHRS is described in detail and its performance is discussed along with the HA-2.The selected PHRS design to be studied is the air-cooled PHRS present in some Gen III/Gen III + VVERs, such as the VVER-1000/V412, the VVER-1200/V392M/V509/V523 and the VVER-TOI. Previous studies have developed isolated Thermal-Hydraulic (TH) models of this air-cooled PHRS, see (Ayhan and Sokmen, 2016a, 2016b; Khubchandani et al., 2013a). Additionally, there are several references on experimental facilities for air-cooled PHRS, see (Berkovich et al., 2006; Elkin et al., 2018; Kopytov et al., 2009, 2011; Morozov et al., 2014; Morozov and Sakhipgareev, 2017; Shlepkin et al., 2020a, 2020b). However, only a few references analyze in detail the effect of the air-cooled PHRS in SBO sequences, both with and without LOCA, see (IAEA, 2012; ROSATOM, 2022).

The present work has been conducted in the framework of the “Integrated Safety Analysis of Modular and Evolutive Reactors” (ISAS-MORE) project. Within this project, accidental sequences (SBLOCA, MBLOCA, LBLOCA, SBO, …) have been analyzed using the TRACE code,

Table 2
PHRS designs comparison.

Reactor design	Reactor Thermal Power (MW)	Number of PHRS trains (HXs/train)	Maximum Heat removal per train (MW)	Connected to	Heat sink	IAEA PSS category
AP1000	3000	1 (1 HX/train)	60	RCS	Water pool	D
BWR/3	1400	1 - 2 (1–2 HX/train)	40	RPV	Water pool	D
BWRX-300	870	3 (2 HX/train)	33	RPV	Water pool	D
ESBWR	4500	4 (2 HX/train)	33	RPV	Water pool	D
HPR-1000 (CGN, CNNC)	3000	3 (N/A)	20	SGs Secondary side	Water pool	D
NuScale	160	2 (1 HX/train)	4	SGs Secondary side	Water pool	D
VVER-1000/V412	3000	4 (3 HX/train)	20	SGs Secondary side	Air flow	D
VVER-1200/V392M	3200	4 (2 HX/train)	30	SGs Secondary side	Air flow	D
VVER-1200/V491	3200	4 (16 HX/train)	30	SGs Secondary side	Water pool	D
KERENA	3370	4 (1 HX/train)	N/A	RCS	Water pool	B

Table 3
Passive Safety Systems IAEA *categories* (Burgazzi, 2012; IAEA, 2009).

Category	Criteria						Examples
	Moving fluids	Moving parts	Signal input	External power	Human initiation	Human interaction	
A	No	No	No	No	No	No	Cooling radiation, concrete building
B	Yes	No	No	No	No	No	Cooling based on natural circulation
C	Yes	Yes	No	No	No	No	Accumulators, check valves
D	Yes	Yes	Yes	No/Yes	No	No	Passive heat removal systems, elevated gravity drain tanks

focusing on the conventional safety systems of Gen II VVER reactors, see (E Redondo-Valero et al., 2023; Redondo-Valero et al., 2024). This includes the verification of the Probabilistic Safety Analysis (PSA) level 1 Event Trees (ET) and the proposal of new ones.

The paper is structured as follows: first, an overview of all passive heat removal systems is given in Section 2. Section 3 then discusses the air-cooled PHRS design selected for analysis and its modeling for the TRACE code; Section 4 shows how the air-cooled PHRS has been incorporated into a plant model for a VVER-1000/V320 reactor. Thereafter, Sections 5, 6 and 7 present the SBO sequence and the SBLOCA/LBLOCA along with SBO sequences respectively simulated with the VVER-1000/V320 plant model incorporating the air-cooled PHRS and the HA-2. The ETs for the Loss Of Offsite Power (LOOP), SBLOCA and LBLOCA sequences is then developed in Section 8, considering the performance of the HA-2 and the air-cooled PHRS. Finally, the conclusions are presented in Section 9.

2. Overview of passive heat removal systems

The PHRSs are designed to remove decay heat from the core over extended periods of time without the need for AC power or human intervention, (Surip et al., 2022). The following section provides an overview of the different types of PHRS designs.

There are different PHRS designs, which are incorporated into several Gen III/Gen III + LWR designs. The PHRSs can be divided into two groups, those that are connected to the secondary side of the SGs and those that are connected to the Reactor Coolant System, (RCS) or the Reactor Pressure Vessel (RPV), see Table 2. That PSSs can also be distinguished according to the heat sink: a large pool of water or the atmospheric air.

- PHRS in the secondary side of the SGs: The PHRSs in the SGs are typically found in a large number of Gen III/Gen III + Pressurized Water Reactors (PWR) designs, both small and large, with some exceptions such as the Westinghouse AP1000 and the CAREM reactors. In this PHRS configuration, the decay heat is removed via a two-phase natural circulation loops connecting elevated Heat Exchangers (HX) to the SGs, (IAEA, 2009). The number of PHRS trains is usually equal to the number of RCS loops. The PHRS in the SGs can be water or air cooled:
  - o **Cooled by a water pool**: The HXs are located in a large pool of water at atmospheric conditions. When the PSS comes into operation, the steam energy from the SGs is transferred to the water pool, which heats up and evaporates. This design is found in the following large reactors: the HPR-1000 (Xing et al., 2016), and the VVER-1200/V491 (Bezlepkin et al., 2014), where the water pool is located in an elevated position between two containment structures. It is also found in small reactors; ACP-100, SMART, RITM-200 (Ekariansyah et al., 2021) and in NuScale, where the tube bundle is located in the external pool where the NuScale power modules are inserted, (NuScale Power LCC, 2020).
  - o **Cooled by air flow**: The HXs are cooled by external atmospheric air. When the PSS is operating, the air passes through the HX tube bundle by natural circulation, increasing its temperature. This design is found in the VVER-1000/V412 (Agrawal et al., 2006) the other VVER-1200 such us V392M (Galiev et al., 2017), V509 and V523. The HXs are housed in a shell between the two containments and are connected to air ducts through which the air flow passes.
- PHRS in the RCS or RPV: The PHRS attached to the RCS or the RPV can be found in the AP1000 and the CAREM PWRs (Bajorek, 2007), and in Boiling Water Reactors (BWR) such as the ESBWR, the BWRX-300 (Rassame et al., 2017) or the conceptual design KERENA (IAEA, 2011). In this PHRS configuration, the decay heat is removed via a HX loop, which can be either a two-phase or a single-phase liquid natural circulation. The HX can be connected directly to the RPV or the RCS, or to another HX within the RPV:
  - o **Cooled by water pool**: The HX, which is placed in a water pool, is connected to the RPV or the RCS. When this PSS comes into operation, the inventory from the core passes into the HX tubes where it causes the water pool to evaporate. In the AP1000 reactor, the HX loop is a liquid single-phase natural circulation loop, but in CAREM and in BWRs, the HX loop is a two-phase natural circulation loop.
    Besides, in the BWR the water-cooled PHRS is referred to as Isolation Condenser (IC). On other hand, it should be noted that not only the Gen III/Gen III + reactors such as the BWRX-300 and the ESBWR have this PSS, but also the Gen II BWR/3 (Dolganov, 2024). However, this design in the Gen II BWR/3 were not developed to withstand an SBO event, so the water pool is considered to be smaller than that of the Gen III/Gen III + LWRs.
  - o **Cooled by a closed extra loop**: The decay heat is removed from the core through a loop containing two HXs, one inside the RPV and one introduced into a pool of water. The main purpose of this design is that the coolant passing through the core does not leave the RPV. This structure is included in some conceptual designs, but no LWR reactor has currently been built with this type of PHRS (Buchholz et al., 2015).

The IAEA establishes a classification to determine how passive a safety system is based on the moving fluids, the moving parts, the signal input, the external power, the human initiation and the human interactions, see (Burgazzi, 2012; IAEA, 2009). Most PHRSs are classified by the IAEA as Category D PSS because they require an input signal to open the isolation valves or the gates that allow the PSS to begin removing decay heat, see Table 3.

In particular, the PHRS in the KERENA reactor design (never built) does not have isolation valves. Heat transfer during normal reactor operation is prevented by an anti-circulation loop which blocks flow between the RPV and the PHRS tubes in stand-by conditions. Therefore, the PHRS for the KERENA reactor does not require signal inputs to start operation and hence is classified as Category B.

It is important to note that not only are some LWRs equipped with PHRS, but other designs, such as liquid metal cooled reactors (IAEA, 1999) and high temperature reactors, also incorporate these PHRS. In Sodium Fast Reactors (SFRs), several designs, including PFR, PFBR, CFBR, BN-1200, JSFR, Kalimer, SPX-1, EFR and ESFR, see (Chetal, 2011; Choi, 2009; Kurisaka, 2012), incorporate air-cooled PHRS, consisting of a closed loop that transfers the decay heat from the reactor pool to the

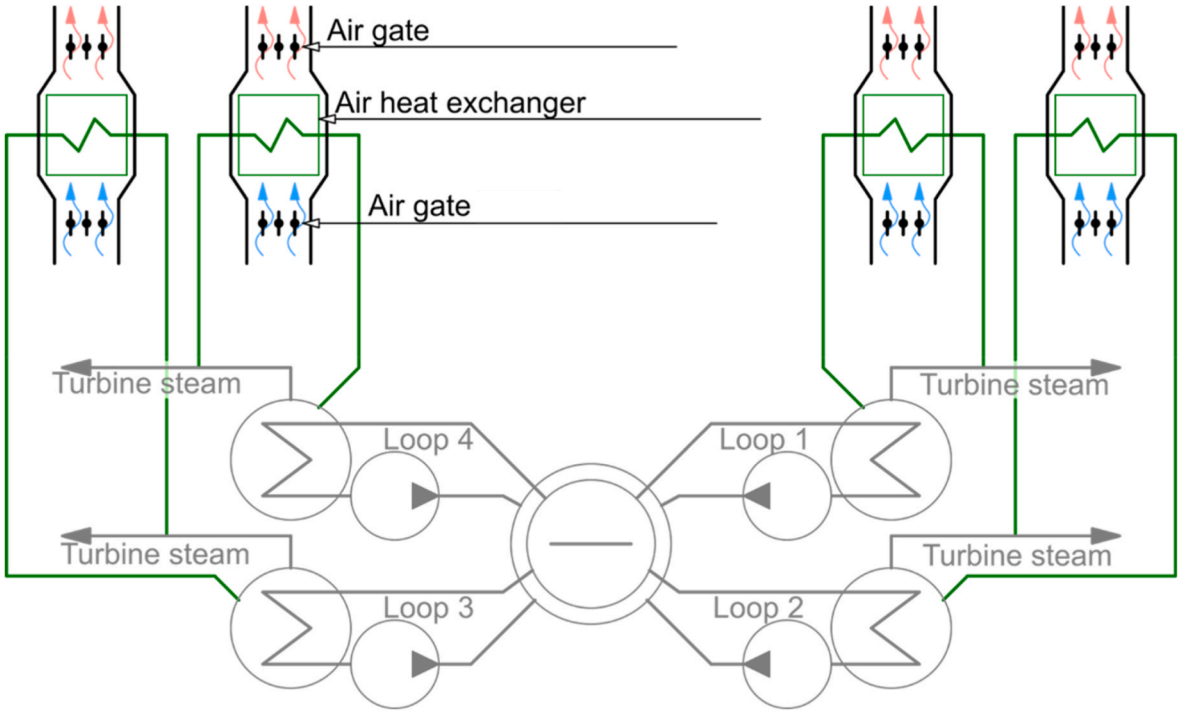

Fig. 1. VVER with air-cooled PHRS.

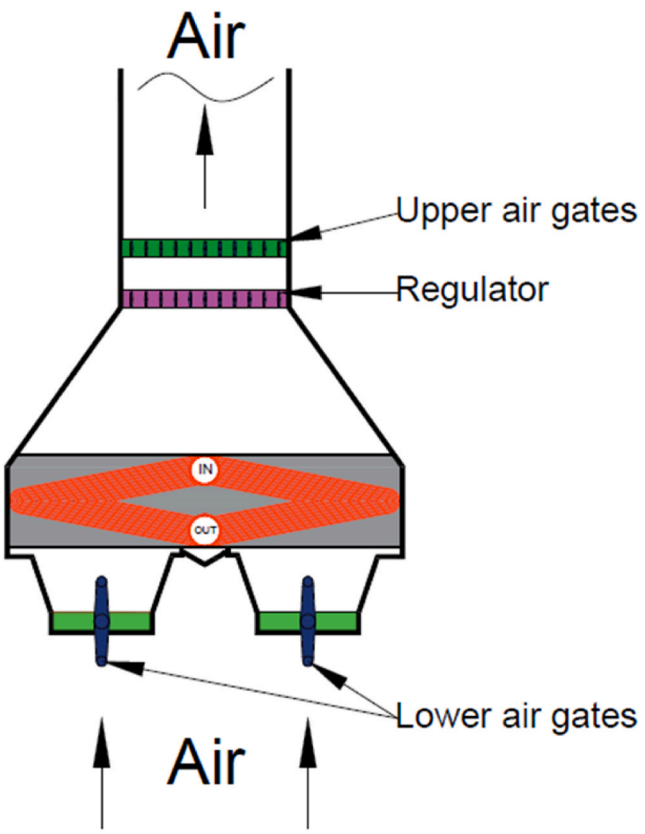

Fig. 2. PHRS heat exchanger, regulator and air gates.

atmosphere. Moreover, the ALMR, PFBR, BN-500, Phenix and Astrid SFRs have air-cooled PHRS, and the Astrid SFR has water-cooled PHRS in the SGs. Furthermore, there are some SFRs, such as the ALMR and the PFR, where the PHRS consists of air flowing around the vessel walls, see (Gluekler, 1997; Jensen and Ølgaard, 1995). On the other hand, it is worth mentioning the HTR-PM, a high-temperature reactor in which the decay heat is transferred from the vessel to the water-filled PHRS tubes by radiation, see (China Nuclear Engineering Group Corporation (CNEC), 2019).

3. Air-cooled PHRS TRACE modeling

The PHRS TH model developed at the UPM corresponds to the air-cooled PHRS present in the VVER-1000/V412, see (Agrawal et al., 2006). This choice was made for two reasons.

1. In addition to simulating SBO sequences, the aim was also to simulate LOCA sequences with SBO, and the Gen III/Gen III + VVER reactors with a long-term passive ECCS, the HA-2, are those which incorporate the air-cooled PHRS.
2. Among the VVER plants with air-cooled PHRS, the one for which the most public information is available is the VVER-100/V412, commissioned at the Kudankulam Nuclear Power Plant (NPP).

Next, the air-cooled PHRS considered in this study is explained. Subsequently, the model of the air-cooled PHRS for the TRACE system code developed at UPM is presented in Section 3.2.

3.1. Description of the air-cooled PHRS

The PHRS incorporated in the VVER-1000/V412 consists of four trains, one per SG, see Fig. 1. Each of the PHRS trains contains 3 HXs, which are located in an elevated position, right where the containment dome begins, (Khubchandani et al., 2013a). It is important to note that in the VVER-1200/V392M, V509, V523 and the VVER-TOI, the air-cooled PHRS also consists of four trains, but each has two HXs instead of three, (Galiev et al., 2017). The design criterion for the air-cooled PHRS in all these reactor designs is that a minimum of 3 out of 4 trains are required to fulfil their safety function, (Ayhan and Sokmen, 2016a).

Each HX is placed in a shell inside an air duct. In the air duct,

Table 4
Air-cooled PHRS geometric data.

Parameter		Value	Units	Reference
Steam lines	Diameter	0.2	m	(Ahmed Pirouzmand and Shahabinejad, 2021; Ayhan and Sokmen, 2015; IAEA, 2009)
PHRS tubes	N° HX	3	–	(Ahmed Pirouzmand and Shahabinejad, 2021; Khubchandani et al., 2013a)
	N° Tubes per HX	630	–	Chaudhary et al. (2017)
	Length	8	m	(Ahmed Pirouzmand and Shahabinejad, 2021; Bharat Heavy Electricals Limited, n.d.; ROSATOM, 2023)
	Height	1.49	m	
Condensate lines	Diameter	0.1	m	Ahmed Pirouzmand and Shahabinejad (2021)
	Height	19.2	m	(Khubchandani et al., 2013a; Kopytov et al., 2009, 2011)
Air ducts	Flow area (Regulator – air duct outlet)	12	m^2	(Bharat Heavy Electricals Limited, n.d.; ROSATOM, 2022; Sri Krishna College of Engineering and Technology (SKCET), 2019)
	Height (Lower air gates – Regulator)	7.5	m	
	Height (Regulator – air duct outlet)	30	m	(Sri Krishna College of Engineering and Technology (SKCET), 2019)

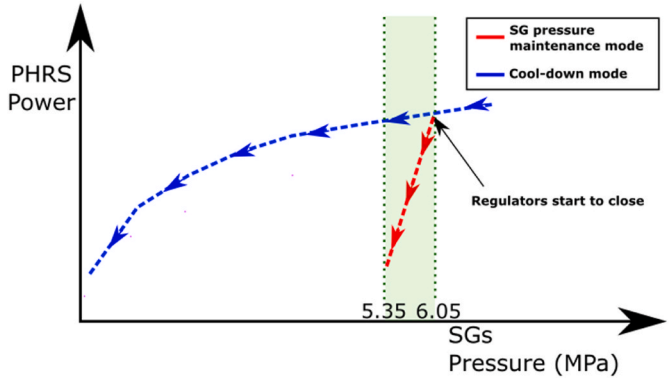

Fig. 3. PHRS power vs. SGs pressure curve in both operating models.

upstream and downstream of the HXs, there are air gates with the capacity to isolate the HXs from the atmosphere, (Agrawal et al., 2006). These air gates have only two positions, closed and open, with no intermediate positions. They remain in the closed position during reactor operation by means of electromagnetic actuators which are de-energized in the event of a loss of AC power, allowing the air gates to open (Agrawal et al., 2006).

Moreover, between the HX and the upstream air gates, there is a regulator consisting of flaps. This regulator is equipped with two actuators, a passive actuator and an active actuator which is powered by the safety class 1 emergency power system (battery powered) (Polunichev et al., 2007).

Each HX contains a steam collector and a condensate collector; the steam collector is located above the condensate collector, see Fig. 2. On the one hand, the steam collector is connected to the condensate collector by a total of 630 horizontal U-shaped tubes with a slight slope, (Chaudhary et al., 2017). On the other hand, the steam collectors and condensate collectors are connected to the SGs thought the steam lines and the condensate lines. The geometric data of the different

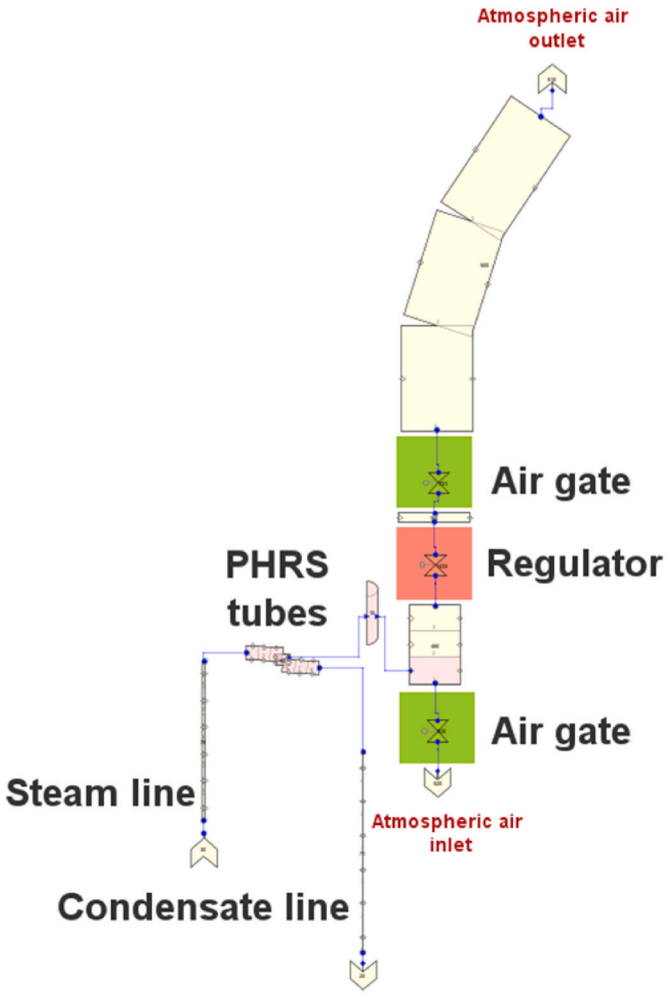

Fig. 4. Air-cooled PHRS (one train) isolate TH model for TRACE code.

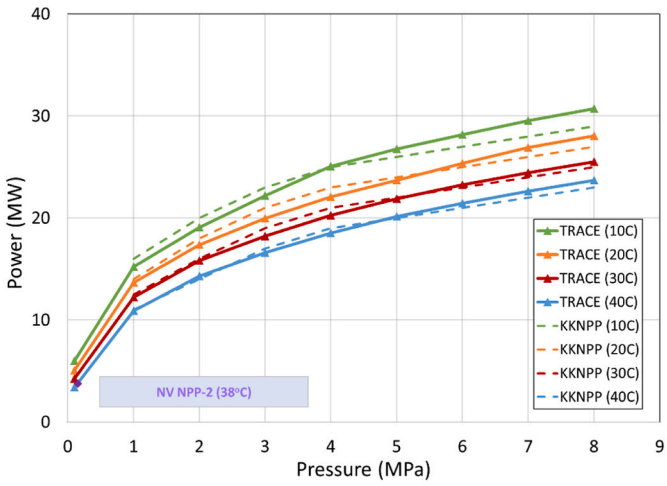

Fig. 5. PHRS power per train vs. SGs pressure (TRACE model).

components of the PHRS are given in Table 4 (Ahmed Pirouzmand and Shahabinejad, 2021; IAEA, 2009; Khubchandani et al., 2013a; Chaudhary et al., 2017; Bharat Heavy Electricals Limited, n.d.; ROSATOM, 2023; Sri Krishna College of Engineering and Technology (SKCET), 2019).

The air-cooled PHRS is designed to remove decay heat for extended

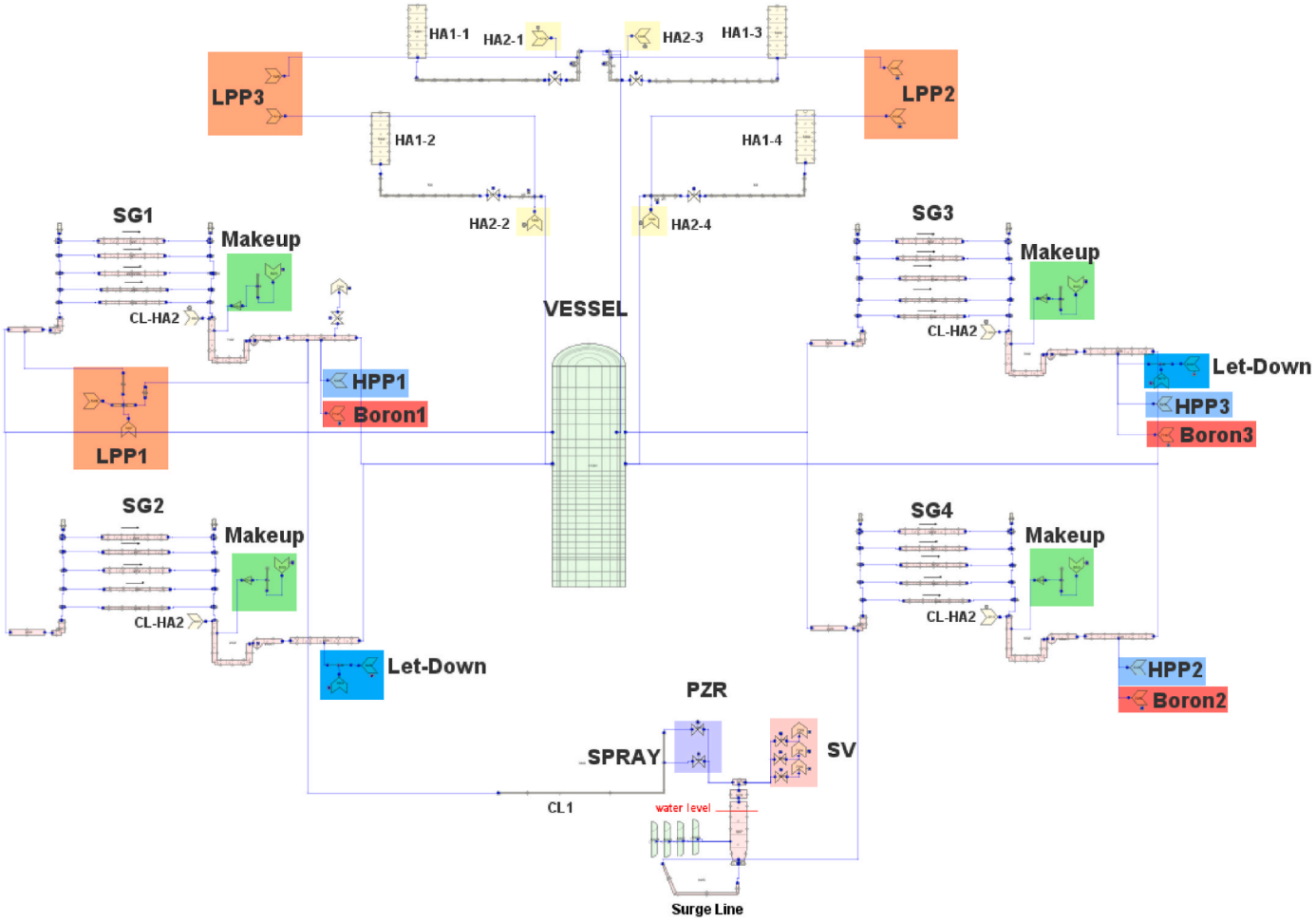

Fig. 6. VVER-1000 RCS including HA-2 system (TRACE model).

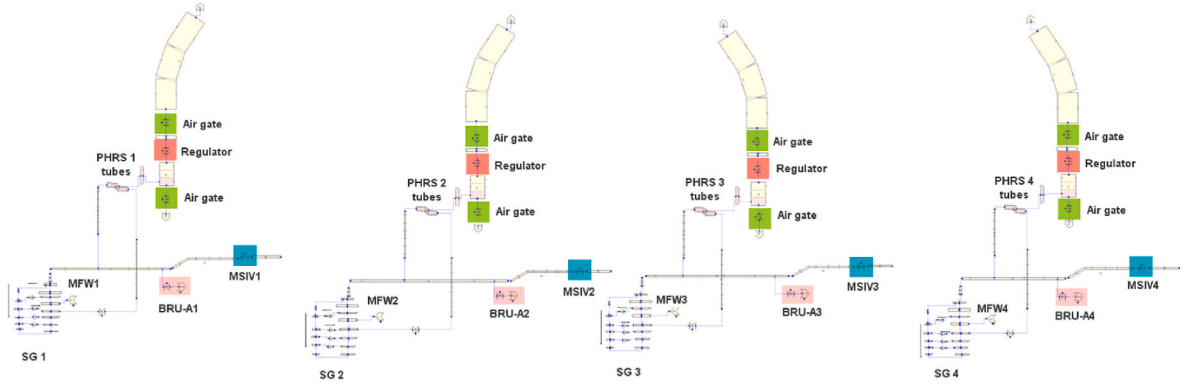

Fig. 7. VVER-1000 Secondary System including the air-cooled PHRS (TRACE model).

periods of time in the event of unavailability of the active heat removal system through the SGs or total loss of AC power, i.e. SBO conditions, (Agrawal et al., 2006; Khubchandani et al., 2013b). Therefore, the air-cooled PHRS should start operating due to (ROSATOM, 2022).

- AC power loss, i.e., SBO conditions.
- A high SGs pressure signal, i.e., SGs pressure above 8.44 MPa.

The electromagnetic actuators of the air gates take 30 s to de-energized, see (Ayhan and Sokmen, 2016a). Moreover, the air gates need 90 s to be fully open, (ROSATOM, 2022).

In addition, the air-cooled PHRS has two operating modes: SGs pressure maintenance mode and RCS cool-down mode, (IAEA, 2012; ROSATOM, 2022).

- SGs pressure maintenance mode: The aim is to remove the decay heat from the core through the SGs by maintaining the pressure of the SGs between 5.35 MPa and 6.05 MPa, (Khubchandani et al., 2013b). This is achieved by controlling the regulator flaps position in the air duct and therefore the air flow through the HX tubes. When, the air-cooled PHRS starts to operate, the regulators flaps are fully open. As the pressure in the SGs drops below 6.05 MPa, the regulators flaps

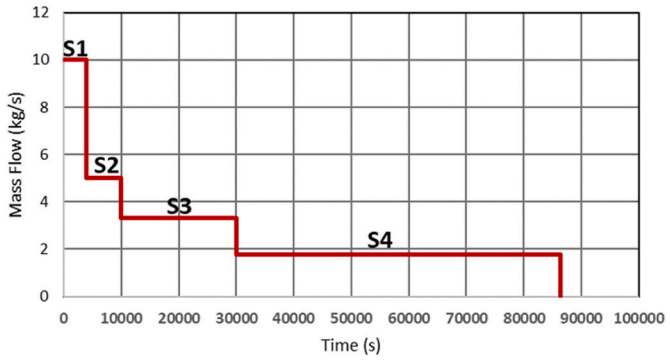

Fig. 8. Second Stage Hydroaccumulators (HA-2) mass flow rate (per HA-2 train).

Table 5
Steady State parameters of the VVER-1000/V320 reactor TRACE model.

Parameter	Reference NPP	TRACEV5P5
Core power [MW]	3010	3010
Lower plenum pressure [MPa]	15.84	15.86
Core outlet pressure [MPa]	15.70	15.74
PZR level [m]	8.70	8.71
CLs temperature [K]	560.85	560.96
HLs temperature [K]	591.55	591.13
Average loop mass flowrate [kg/s]	4456	4457
SG outlet pressure [MPa]	6.27	6.27
MFW mass flowrate [kg/s]	409	408
MFW temperature [K]	493	493
SG level [m]	2.50	2.50

Table 6
Main events in the SBO sequence [with PHRS].

Event	Time (s)
SBO (SCRAM, MFW pump and RCPs trip, TT, loss of the condenser, CVCS)	300
BRU-A opening (SL pressure >7.25 MPa)	310
Air gates opening (SBO + 30 s delay)	330
PHRS full capacity (90 s opening)	420
BRU-A closed (SL pressure <6.67 MPa)	490
PHRS regulator starts to close (P_{SG} = 6.05 MPa)	1465
End simulation (24 h)	86400

begin to close, reducing the power that the PHRS can dissipate compared to the power it could remove if the regulators flaps were fully open, see the red line in Fig. 3.

This operating mode is controlled by the passive actuator of the regulator flaps which operates by means of a spring-operated piston system. The piston is driven both by the steam pressure on the secondary side of the SG and by the spring force. The direction of movement of the piston rod, and therefore whether the regulator flaps open or close, is determined by the balance between the SGs steam pressure and the spring force, (Galiev et al., 2017; Polunichev et al., 2007).

- RCS cool-down mode: If the SBO sequence or the loss of the active heat removal systems is followed by a LOCA, the PHRS operates in RCS cool-down mode. When the subcooling margin in the Hot Legs (HL) is below 8 °C, (ROSATOM, 2022), the control that regulates the regulator flaps position is inhibited, forcing them to remain fully open. In this model, the air-cooled PHRS behavior is characterized by a power vs. SG pressure curve, see Fig. 3.

The active actuator of the regulator flaps is responsible for overriding the passive actuator to keep the regulator flaps fully open (Galiev et al., 2017; Polunichev et al., 2007), without the need for human intervention. In addition, if necessary, the active actuator can also be operated by the operator to switch to the RCS cool-down mode (Asmolov, 2011; Turkish Atomic Energy Authority, 2018).

In stand-by mode, the HXs are isolated from the atmosphere by the air gates located both upstream and downstream of the HXs. Otherwise, the regulators flaps are fully open, (ROSATOM, 2022). Moreover, the steam lines and the condensate lines are open, allowing the PHRS tubes to be at SG pressure, (Agrawal et al., 2006; IAEA, 2012).

On the other hand, it is important to note that the Gen III/III + designs of VVER reactors incorporating the air-cooled PHRS do not have passive containment cooling safety systems. Passive containment cooling safety systems are found in the Gen III/III + designs of VVER reactors incorporating the water-cooled PHRS, such as the VVER-1200/V529, the VVER-1200/V527 and the VVER-1200/V491 (Queral et al., 2021).

3.2. PHRS model for the TRACE code

As a first step, an isolated model of the air-cooled PHRS has been developed for the TRACE system code. As the four PHRS trains are symmetrical, only one of them has been developed with boundary conditions in the steam line inlet and the condensate line outlet and the atmospheric air inlet and outlet. The geometric data, the actuation signals and the operating modes included in the TH model are those shown in Section 3.1. The TH model includes the air ducts from the air inlet to the outlet, the U-tube of the HXs, the steam lines and the condensate lines, see Fig. 4.

- **Air duct**: the three air ducts of each train have been modeled in a single one. In the model, the air ducts can be differentiated into three sections modeled with a PIPE component each:

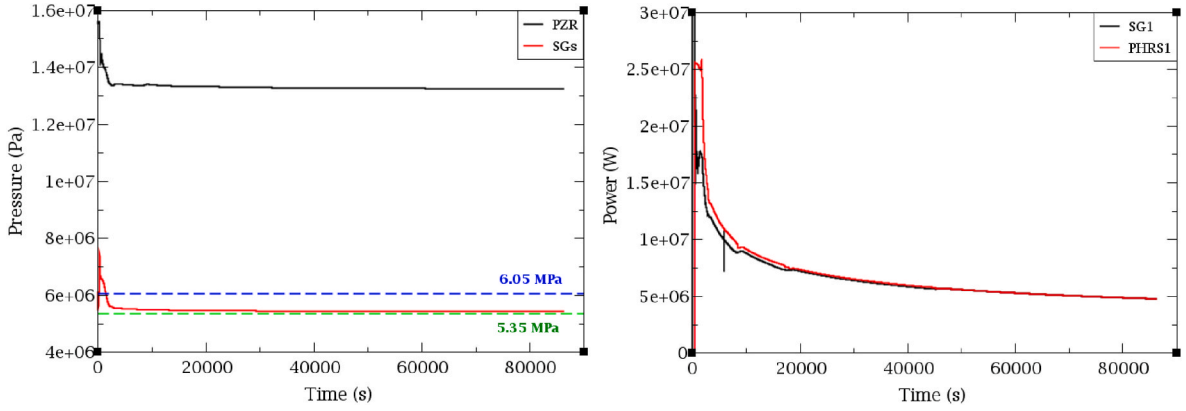

Fig. 9. RCS and SGs pressure (left) and PHRS 1 vs. SG 1 power (right); SBO sequence.

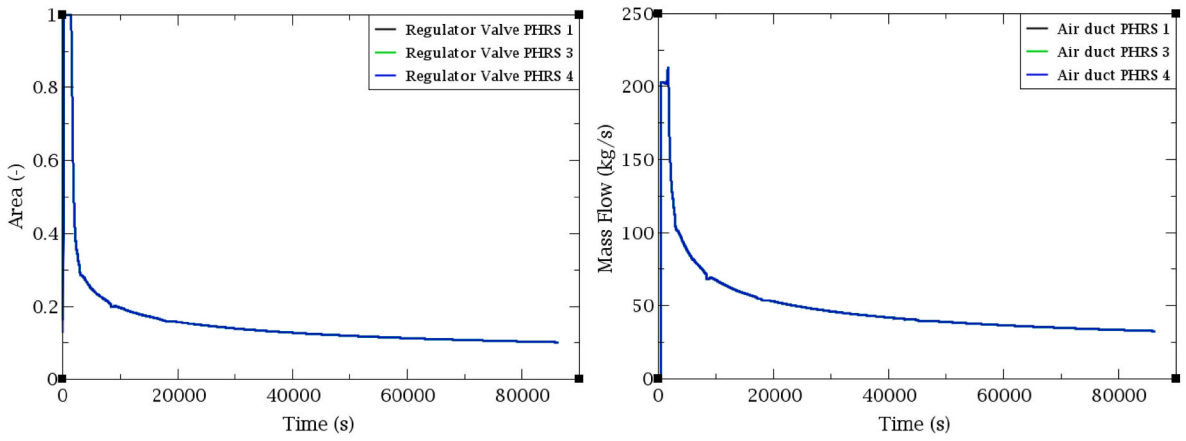

Fig. 10. PHRS Regulators area fraction (left) and PHRS air duct mass flow rate per train (right); SBO sequence.

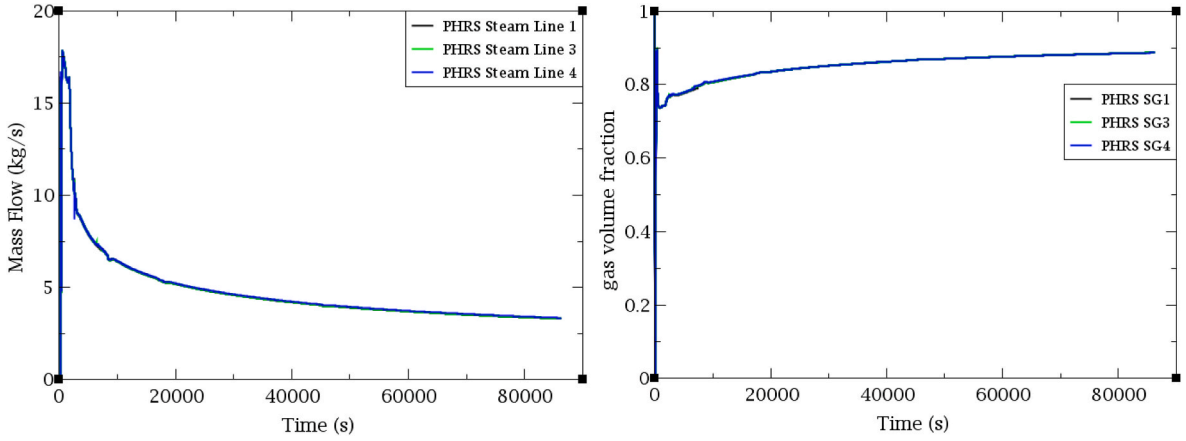

Fig. 11. PHRS steam lines mass flow rate (left) and PHRS outlet bundle tubes void fraction (right); SBO sequence.

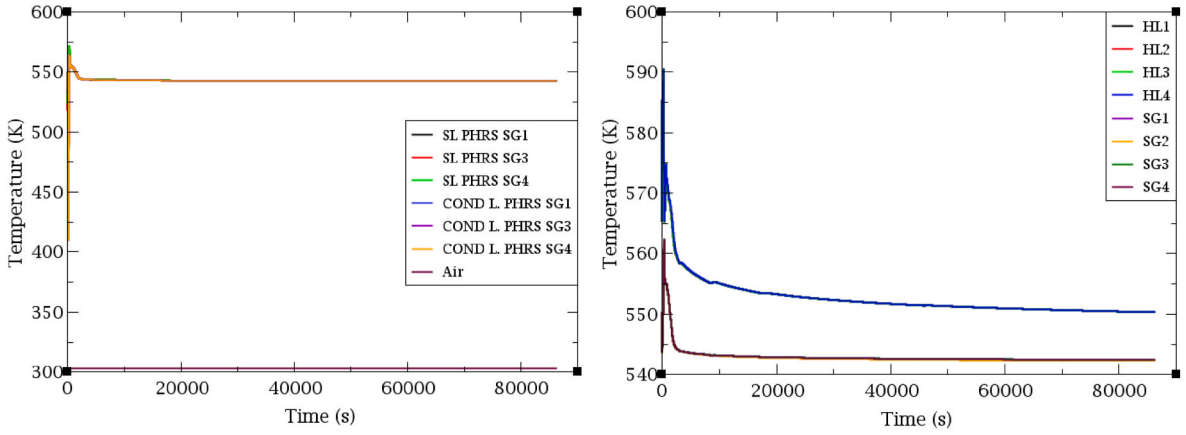

Fig. 12. PHRS steam lines and condensate lines temperature (left) and HLs and outlet SGs temperatures (right); SBO sequence.

- o Air duct between the upper air gates and the atmosphere.
- o Air duct between the upper air gates and the regulator.
- o Air duct between the regulator and the lower air gates. Here is the HEAT-STRUCTURE coupled to the PIPE where the heat transfer to the SGs takes place.

The inlet and outlet of the air duct have been modeled using pressure boundary conditions. In a first calculation of the pressure drop, the difference in height between the air duct inlet and outlet and the air density were taken into account. The pressure difference was then further adjusted to avoid generating a non-zero air flow in the absence of a heat source in the PHRS.

- **PHRS Tube bundle**: The tube bundle has been modeled with a single PIPE component, with three slopes to properly reproduce the U-shape of the pipes. In the available references it has been found that the tubes diameter of the PHRS is around 0.03 m, so this has been

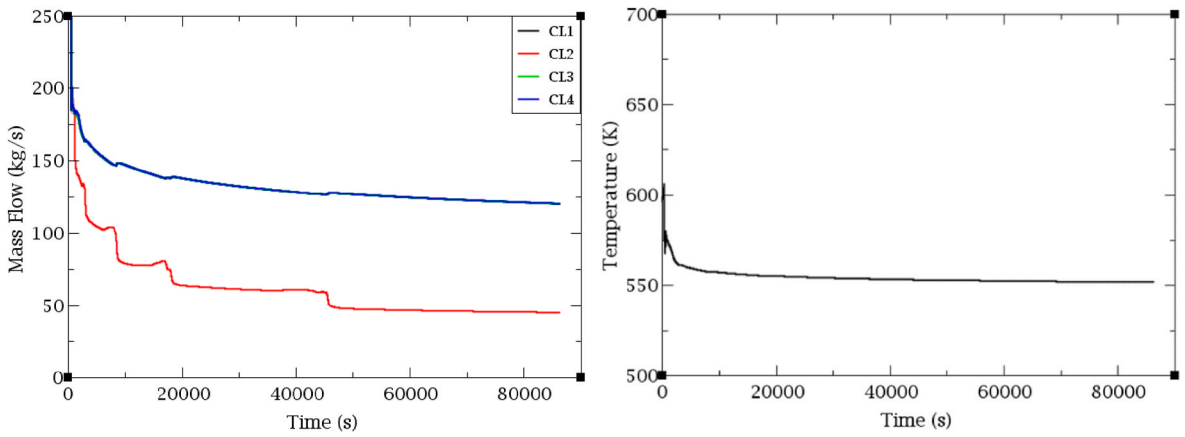

Fig. 13. RCS mass flow rate (left) and Peak Cladding Temperature (right); SBO sequence.

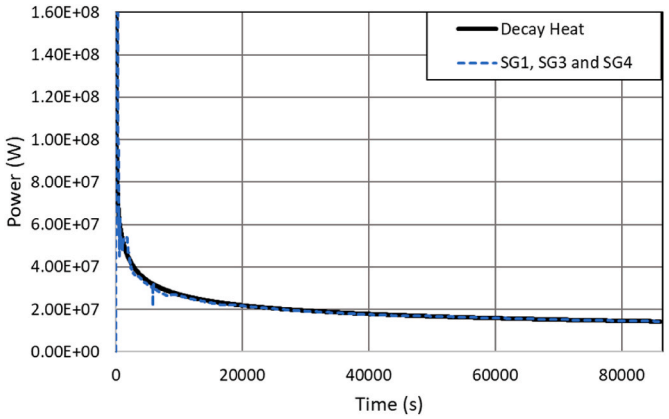

Fig. 14. Heat removal capacity of the PHRS vs. decay heat (SBO sequence).

chosen as the tubes diameter for the TH model, see (Ma et al., 2021; Yücehan-Kutlu, 2019).

The heat transfer between the PHRS tube bundle and the air duct has been modeled using a HEAT STRUCTURE with cylindrical geometry. The inner surface is connected to the PIPE component that represents the PHRS tube bundle, while the outer surface is linked to the first cell of the PIPE modeling the air duct between the regulator and the lower air gates. This HEAT STRUCTURE follows the nodalization of the PIPE representing the PHRS tube bundle, consisting of eight cells with a one-to-one connection.

- **Steam lines and Condensate lines:** both lines have been modeled using PIPE components, with each PIPE divided into six cells.

In the TRACE model, the air gates are controlled by two signals which cause them to open: SBO conditions and SG pressure above 8.44 MPa. The opening of the air gates allows the air to pass through the air ducts, which leads the PHRS to start operation. On the other hand, the area of the regulator is determined by a control that maintains the SG pressure between 5.35 MPa and 6.05 MPa, as follows.

- When the SGs pressure is above 6.05 MPa, the regulators are fully open.
- When the SG pressure starts to drop below 6.05 MPa, the regulators start to close.
- When the SGs pressure drops below 5.35 MPa, the regulators close completely.

In addition, an HLs subcooling signal has also been implemented on the TH model, which forces the regulators to remain fully open, overriding the regulator area control. In this way it is possible to switch from SG pressure maintenance mode to RCS cool-down mode.

To verify the performance of the air-cooled PHRS model developed at the UPM, the power that a train can remove at different pressures was determined. The results obtained were then compared with the results from the FSAR code for an isolated PHRS model of the Kudankulam NPP (Khubchandani et al., 2013a). In order to have a comprehensive view of the behavior of the PHRS under different outdoor conditions, the PHRS power vs. pressure curves have been obtained for various air temperatures: 10 °C, 20 °C, 30 °C and 40 °C, see Fig. 5.

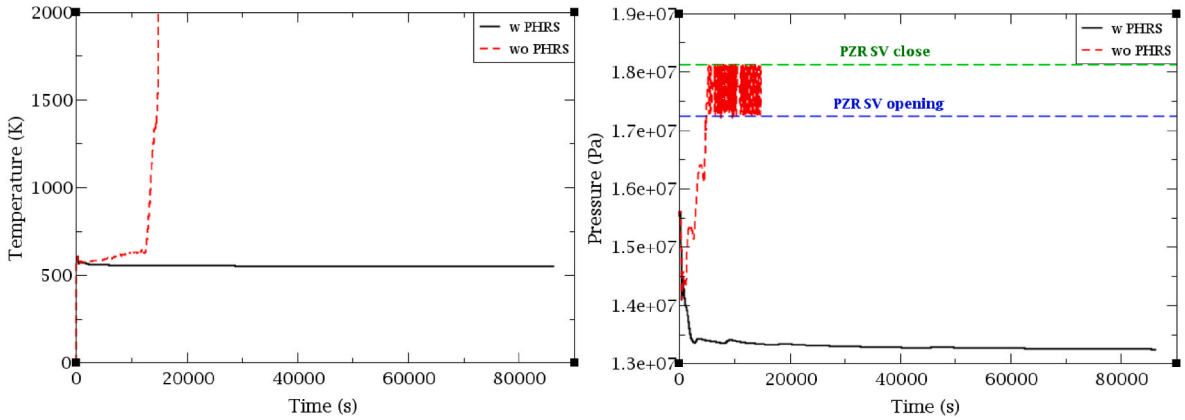

Fig. 15. PCT (left) and RCS pressure (right); SBO sequence with HA-2 and PHRS, with HA-2 and without PHRS, without PHRS and with HA-2.

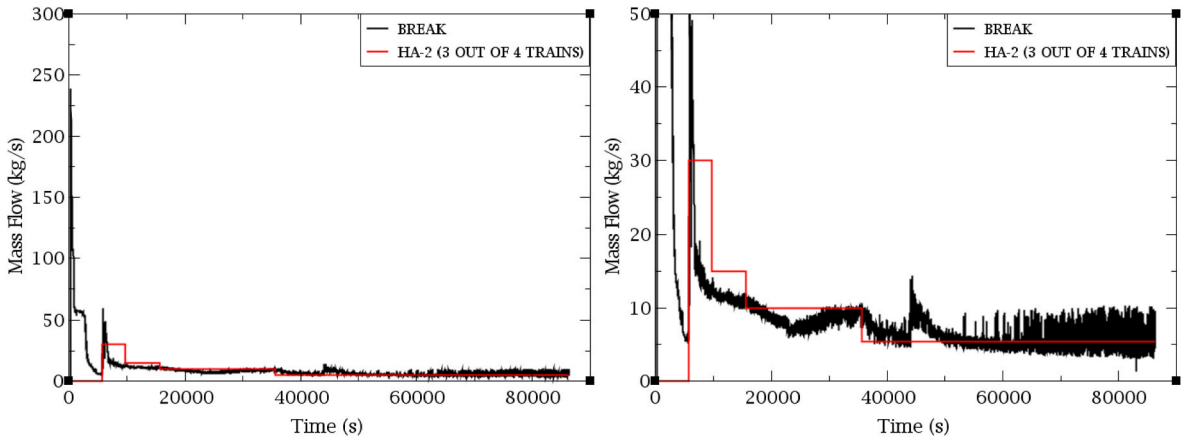

Fig. 16. Break mass flow rate (left) and Break mass flow rate (y-axis zoomed in) (right); SBLOCA (2 inches) along with SBO sequence.

Table 7
Main events in the SBLOCA (2 inches) along with SBO sequence (with PHRS and HA-2).

Event	Time (s)
SBLOCA along with SBO (SCRAM, MFW pumps and RCPs trip, TT, loss of the condenser, CVCS off)	300
BRU-A opening (SL pressure >7.25 MPa)	310
Air gates opening (SBO + 30 s delay)	330
PHRS full capacity (90 s opening)	420
Signal for PHRS in cooldown mode (T_{sat} –T_{HL} < 8 °C)	485
BRU-A closed (SL pressure <6.67 MPa)	540
HA-1 injection begins (RCS pressure <6 MPa)	2275
MSIV close (SG pressure <4.69 MPa)	2460
HA-2 injection set point (RCS pressure <1.5 MPa)	5640
First stage HA-2 injection begins (HA-2 set-point + 100 s)	5740
HA-1 injection ends (HA-1 empty)	7211
Second stage HA-2 injection begins (HA-2 set-point + 4000 s)	9640
Third stage HA-2 injection begins (HA-2 set-point + 10000 s)	15640
Fourth stage HA-2 injection begins (HA-2 set-point + 30000 s)	35640
End simulation (24 h)	86700

Each curve has been obtained for a total of nine pressure values, from 8 MPa to 0.1 MPa. It is noteworthy that the TRACE model curves are very close to the Kudankulam curves from 8 MPa to 1 MPa. The value for atmospheric pressure at Kudankulam NPP is not available in (Khubchandani et al., 2013a), but it can be found in (Kopytov et al., 2009), that the power for a pressure of 0.15 MPa is about 15 MW for an outside temperature of 38 °C at the Novovoronezh NPP, which is about 3.75 MW per train, see Fig. 5.

4. VVER-1000/V320 with PSSs model

The PHRS model, previously presented in Section 3, has been implemented in a TH model for the TRACEV5P5 code (NRC, 2017) of a VVER-1000/V320 reactor, see Figs. 6 and 7. The nodalization of the full plant model was built based on a VVER-1000/V320 RELAP5 model, (Sanchez-Espinoza and Bottcher, 2006), and has been applied for MB/LBLOCA and SBLOCA analyses in previous studies, see (Elena Redondo-Valero et al., 2023; E Redondo-Valero et al., 2023; Redondo-Valero et al., 2024).

The TRACE model of the VVER-1000 reactor also includes the HA-2 system, a passive low-pressure ECCS connected downstream to the First Stage Hydroaccumulator (HA-1) discharge lines and upstream to the Cold Legs (CL). The HA-2 system consists of four trains of 33 % capacity each and two 120 m^3 tanks which inject borated water into the RCS in four stages, see Fig. 8 and (ROSATOM, 2022), when the RCS pressure is below 1.5 MPa. The HA-2 actuation signal has a delay of 100 s. A mass flow rate boundary condition has been used to model each of the four trains (i.e. the injection mass-flow rate from both tanks of each train). This approach was taken because of the lack of sufficient information in public references to accurately model the system using TH components.

In the TH model, the line connecting the top of the HA-2 to the CLs has been modeled. This line opens when the HA-2 set-point is reached, allowing the HA-2 to remain at RCS pressure. This causes some of the inventory from the CLs to be drawn into the HA-2. The inventory sucked in is equal to the volume flow rate being injected by the passive low-pressure ECCS. Therefore, the mass flow rate sucked in by the upper lines of the HA-2 is the volumetric flow rate being injected by the HA-2 per the density of the CLs inventory.

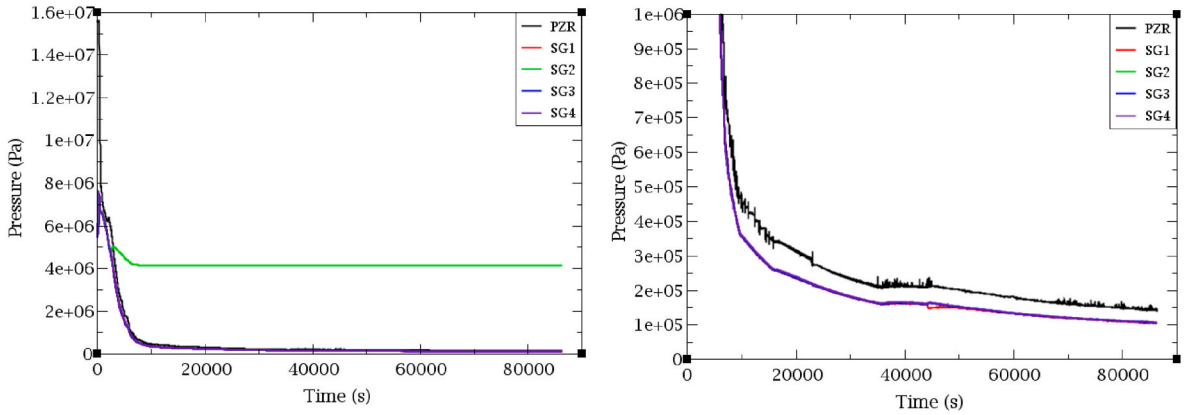

Fig. 17. RCS and SGs pressure (left) and RCS and SGs pressure (y-axis zoomed in) (right); SBLOCA (2 inches) along with SBO sequence.

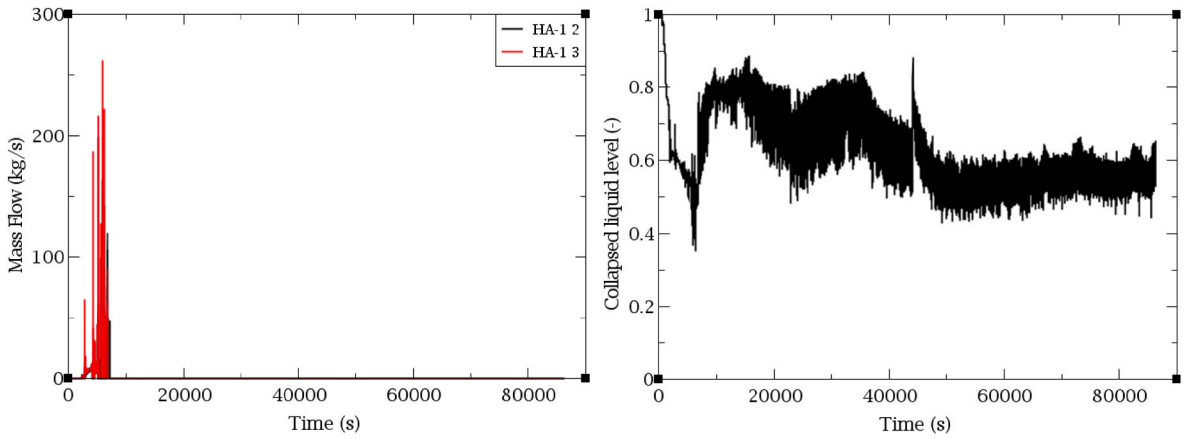

Fig. 18. HA-1 mass flow rate (left) and core collapsed liquid level (right); SBLOCA (2 inches) along with SBO sequence.

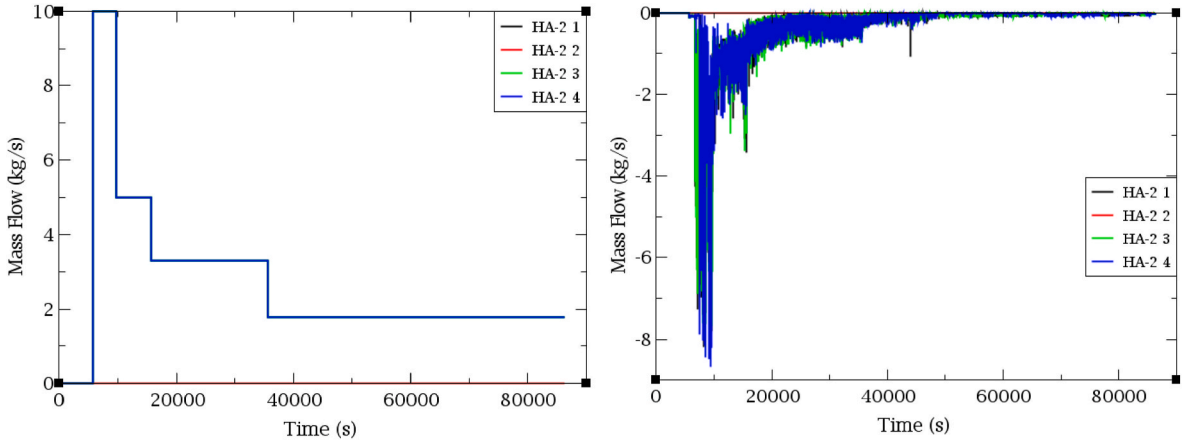

Fig. 19. HA-2 mass flow rate (left) and HA-2-CLs line mass flow rate (right); SBLOCA (2 inches) along with SBO sequence.

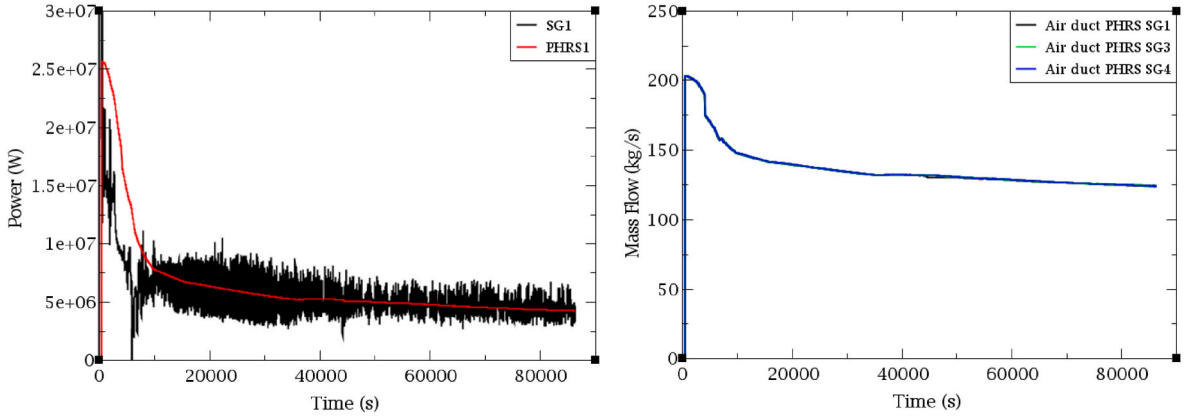

Fig. 20. PHRS 1 vs. SG 1 power (left) and PHRS air duct mass flow rate per train (right); SBLOCA (2 inches) along with SBO sequence.

Moreover, the full plant TH model encompasses actuation signals for the active ECCS, the Steam Dump Valves to the Containment (BRU-A), the steam lines safety valves, the Main Steam Isolation Valve (MSIV) (also known as BZOK valves), the Steam Dump Valves to the Condenser (BRU-K), the Steam Dump Valves to the Atmosphere (BRU-SN), the pressurizer (PZR) heaters, spray and safety valves, the Emergency Boron Injection System (EBIS), and the HA-1 isolation valves. Additionally, the model includes signals for the SCRAM, the Reactor Coolant Pump (RCP) trip, the Turbine Trip (TT), the Main Feedwater (MFW) pumps trip, and the Emergency Feedwater (EFW) pumps startup.

Therefore, the final TH model used in this study includes a total of 441 TH components, 460 signal variables, 335 control blocks, and 313 trips. The full plant TH model has been validated under steady-state conditions using data from a VVER-1000/V320 NPP, see (Kolev et al., 2006). The values obtained are close to the reference plant data, see Table 5.

5. Performance of the PHRS during an SBO sequence

The aim of this section is to analyze the behavior of the air-cooled

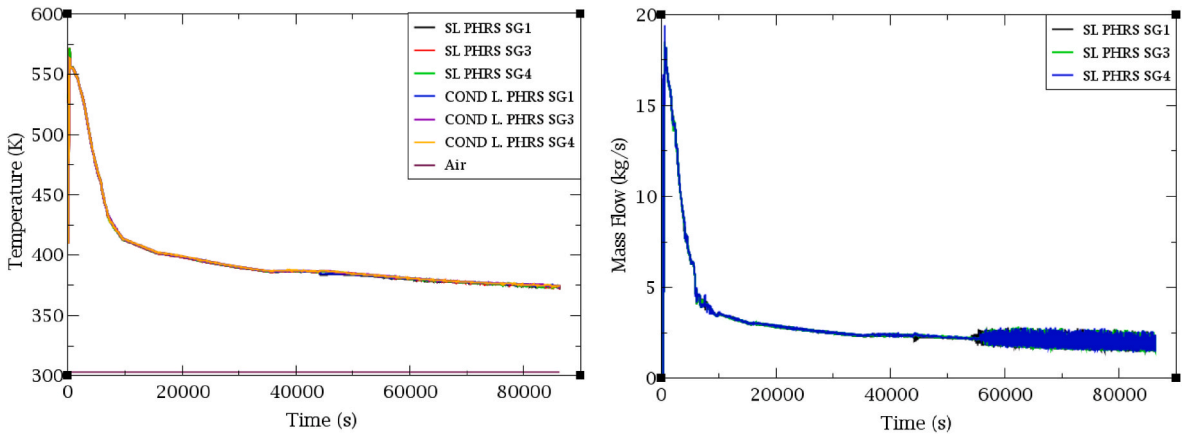

Fig. 21. PHRS steam lines and condensate lines temperature (left) and PHRS steam lines mass flow rate (right); SBLOCA (2 inches) along with SBO sequence.

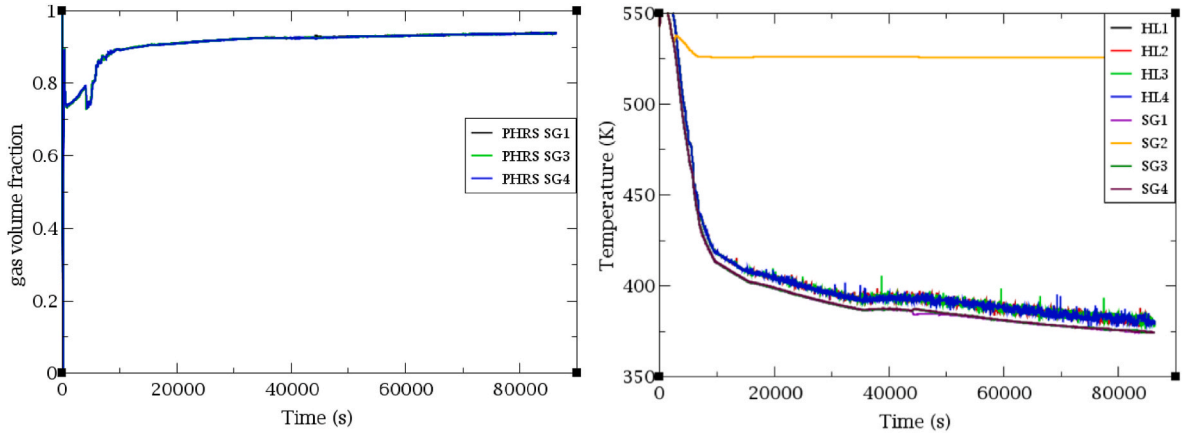

Fig. 22. PHRS outlet bundle tubes void fraction (left) and HLs and outlet SGs temperatures (right); SBLOCA (2 inches) along with SBO sequence.

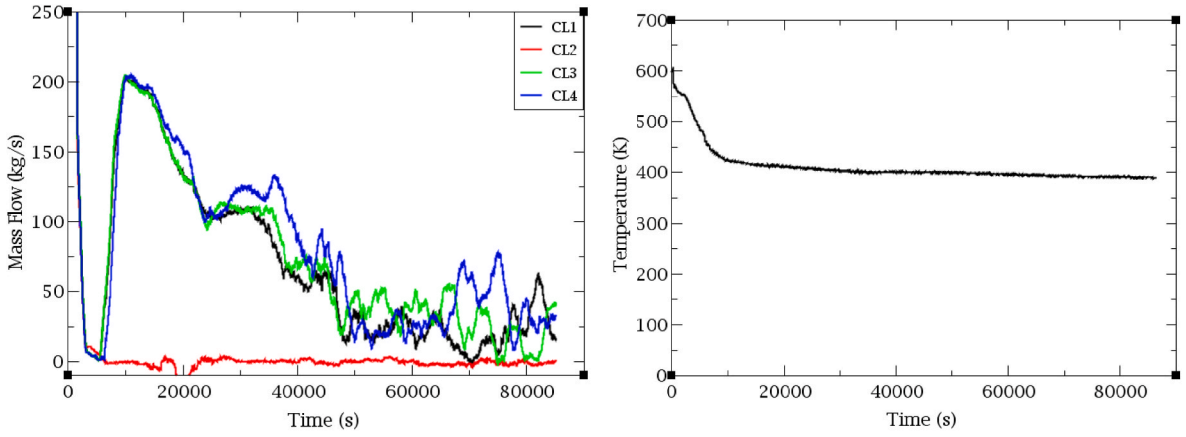

Fig. 23. RCS mass flow rate (left) and Peak Cladding Temperature (right); SBLOCA (2 inches) along with SBO sequence.

PHRS when operating in SG pressure maintenance mode during an SBO sequence. It should be noted that this sequence is analyzed only for the VVER-1000/V392 design in (IAEA, 2012), both considering and not considering the air-cooled PHRS performance, and for the VVER-1200 in (ROSATOM, 2022).

In the present work, the sequence has been analyzed taking into account the air-cooled PHRS Success Criterion (SC) of 3 out of 4 trains, i.e., the trains connected to SGs 1, 3, and 4 are available, while SG 2 is unavailable. In addition, this analysis does not consider the potential leakages of the RCS inventory through the RCPs. It is important to note that a large number of operating NPPs, both Gen II and Gen III/III+, have passive thermal shutdown seals (or hydrodynamic seals) on the RCPs to prevent leakage of the RCS inventory through the RCPs in the SBO sequence. Furthermore, the SBO sequence with RCPs leakages is covered by the SBLOCA with SBO analysis as shown in Section 6.

In Section 5.1, the SBO sequence is first analyzed taking into account the availability of the air-cooled PHRS. Subsequently, in Section 5.2, it is analyzed how long it would take for the sequence to reach Core Damage

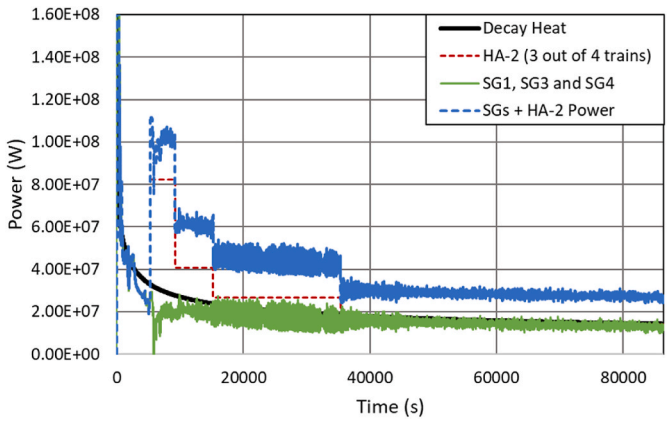

Fig. 24. Heat removal capacity of the HA-2 and PHRS vs. decay heat in the SBLOCA (2inches) along with SBO sequence.

(CD) if the PHRS operation is not considered.

5.1. SBO sequence with PHRS available

The SBO sequence starts after 300 s of steady state. At that instant there is a total loss of AC power, failure to start of the Emergency Diesel Generators (EDG), reactor SCRAM, RCPs trip, loss of the CVCS, MFW pumps trip, TT and loss of the condenser. The evolution of the main events during this sequence is shown in Table 6.

At the beginning of the sequence, the SGs pressure starts to rise, but the condenser relief valves, BRU-K, do not open as the condenser is lost. Therefore, the SGs pressure continues to rise until it reaches the set point of the steam line relief valves, BRU-A, see Fig. 9 (left). Within 30 s of the AC power loss signal, the air gates begin to open, both upstream and downstream of the PHRS HXs. The three available PHRS trains are at 100 % capacity 90 s later, see Fig. 9 (right). Due to the action of the PHRS, the pressure in the SGs starts to decrease, which causes the BRU-A valves to close. At 1465 s, the pressure in the SGs drops below 6.05 MPa, causing the air-cooled PHRS regulator to begin closing (by means of the passive actuator), see Fig. 10 (left).

By gradually closing the regulators, the air flow in the air ducts is passively regulated. It is observed that the air flow per air-cooled PHRS train is about 200 kg/s at the beginning of the sequence, decreasing to around 30 kg/s after 24 h, Fig. 10 (right). This air flow (at 303.15 K) allows the extraction of a power between 25 MW at the beginning of the sequence and 5 MW after 24 h per train of the air-cooled PHRS, see Fig. 9 (right). Note also that the heat removed from the RCS by the SGs is less than that removed by the PHRS tubes at the beginning of the sequence, but in the long term the two become equal.

In the steam and the condensate lines of the air-cooled PHRS, it is possible to observe how the heat transfer between the secondary side of the SGs and the air establishes a natural circulation of about 4 kg/s after 24 h of the sequence, see Fig. 11 (left). Furthermore, it can also be observed that the void fraction at the outlet of the PHRS tubes is 90 %, see Fig. 11 (right), causing a mixture of steam and saturated liquid at a temperature of 540 K to return to the SGs, Fig. 12 (left).

Moreover, SGs inventory, which is at saturation, has a lower temperature than the liquid in the HLs, see Fig. 12 (right). This cooling leads natural circulation in the RCS of about 125 kg/s for each of the three loops with the available PHRS. In loop 2, where the PHRS is not operational, there is a gradual loss of natural circulation, Fig. 13 (left).

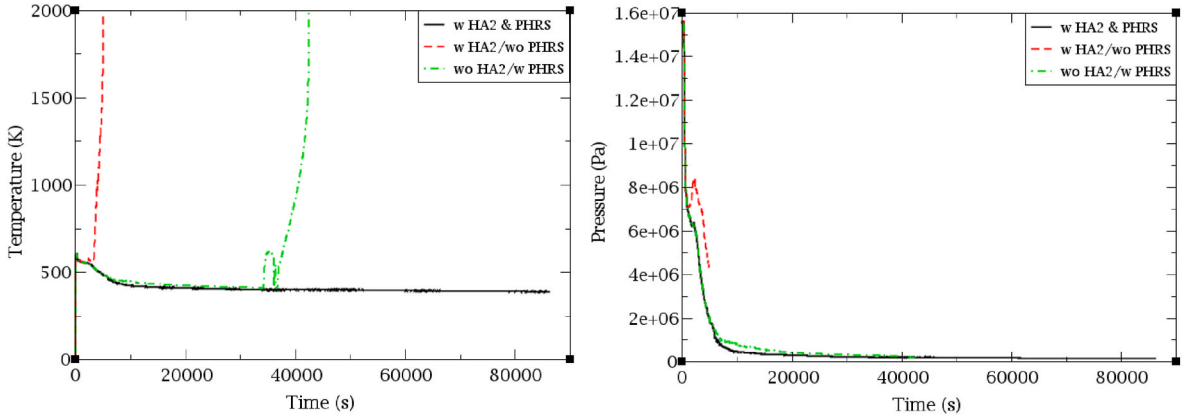

Fig. 25. PCT (left) and RCS pressure (right); SBLOCA (2 inches) sequence with HA-2 and PHRS, with HA-2 and without PHRS, without PHRS and with HA-2.

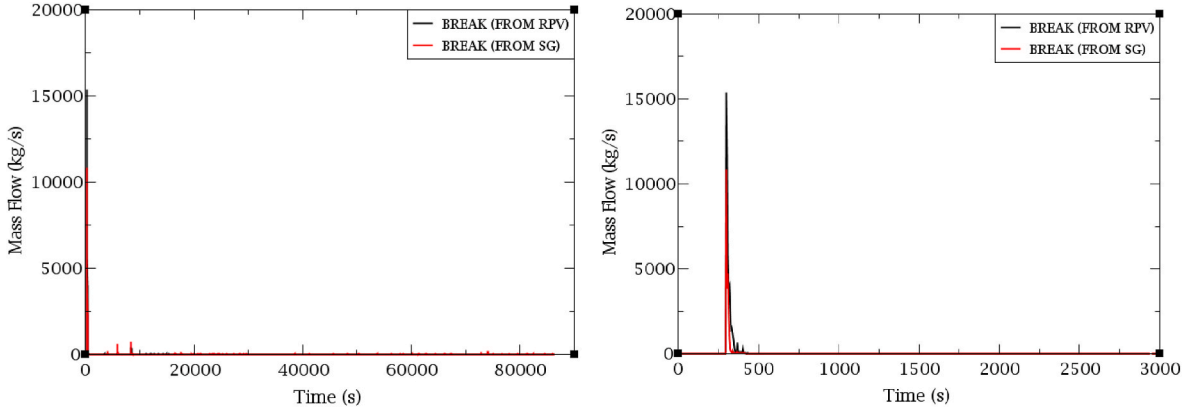

Fig. 26. Break mass flow rate (left) and Break mass flow rate (x-axis zoomed in) (right); DEGB LBLOCA along with SBO sequence.

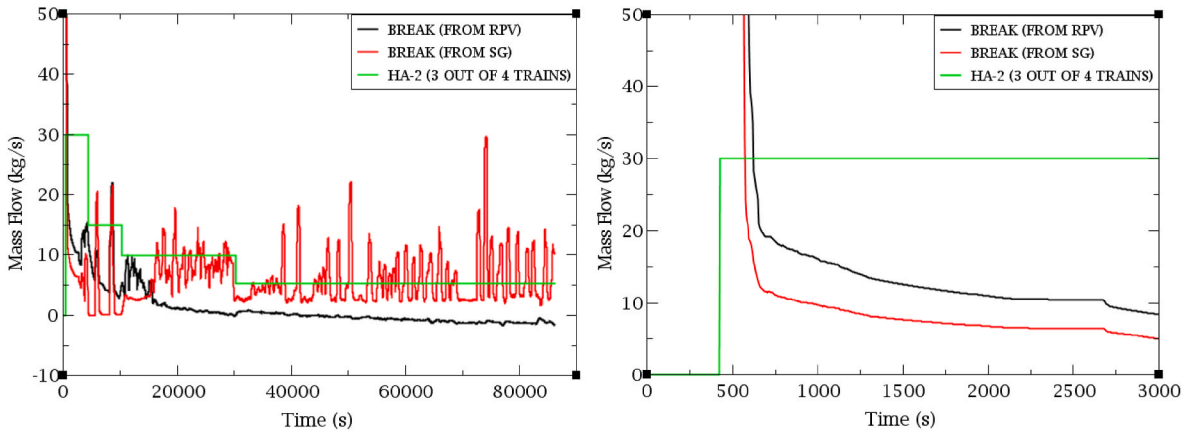

Fig. 27. Break vs. HA-2 mass flow rate (y-axis zoomed in) (left) and break vs. HA-2 mass flow rate (x-axis and y-axis zoomed in) (right); DEGB LBLOCA along with SBO sequence.

Table 8
Main events in the DEGB LBLOCA along with SBO sequence [with PHRS and HA-2].

Event	Time (s)
LBLOCA along with SBO (SCRAM, MFW pumps and RCPs trip, TT, loss of the condenser, CVCS off).	300
Signal for PHRS in cooldown mode (T_{sat} –T_{HL} < 8 °C)	305
HA-1 injection begins (RCS pressure <6 MPa)	315
HA-2 injection set-point (RCS pressure <1.5 MPa)	325
Air gates opening (SBO + 30 s delay)	330
HA-1 injection ends (HA-1 empty)	420
PHRS full capacity (90 s opening)	420
First stage HA-2 injection begins (HA-2 set-point + 100 s)	425
MSIV close (SG pressure <4.69 MPa)	495
Second stage HA-2 injection begins (HA-2 set-point + 4000 s)	4325
Third stage HA-2 injection begins (HA-2 set-point + 10000 s)	10325
Fourth stage HA-2 injection begins (HA-2 set-point + 30000 s)	30325
End simulation (24 h)	86400

It can thus be concluded that the performance of 3 out of 4 air-cooled PHRS trains enables the control of pressure in both the RCS and the SGs without the need for human actions or the intervention of any other safety system. It is noteworthy that the decay heat removed by the SGs, due to the air-cooled PHRS performance, becomes equivalent to the core thermal power, Fig. 14. This ensures that the Peak Cladding Temperature (PCT) in the core does not increase during the first 24 h of the sequence, see Fig. 13 (right).

5.2. SBO sequence with PHRS unavailability

The aim of this section is to analyze how the SBO sequence evolves without the air-cooled PHRS performance, in order to know how long it would take for the sequence to find the CD if the PSS is not taken into account.

The results show that when the PHRS is not available, the SGs act as a cold source as long as they have some inventory. Once they are empty, the capacity to remove the decay heat through the SGs is lost, so the RCS pressure increases until it reaches the set point of the PZR relief valves, Fig. 15 (right). From this point on, the RCS inventory starts to be lost, leading to core uncovering at around 15000 s and finally to the CD a few minutes later, Fig. 15 (left).

In summary, it can be observed that without the PHRS performance, the inventory of the SGs and subsequently the PZR relief capacity are able to maintain the core temperature below 1477 K for at least 4 h. After this time, if the air-cooled PHRS is not available, the SBO sequence reaches CD.

6. Performance of the PHRS and HA-2 in SBLOCA along with SBO sequences

The aim of this section is to determine the performance of the air-cooled PHRS in RCS cool-down mode during an SBLOCA sequence under SBO conditions. Similar sequences have been analyzed for VVER-1200 designs (ROSATOM, 2022). In addition, three SBLOCA experiments with SBO were performed in the PSB experimental facility with a VVER-TOI configuration, see (Elkin et al., 2018).

In order to determine the containment pressure in this sequence, the

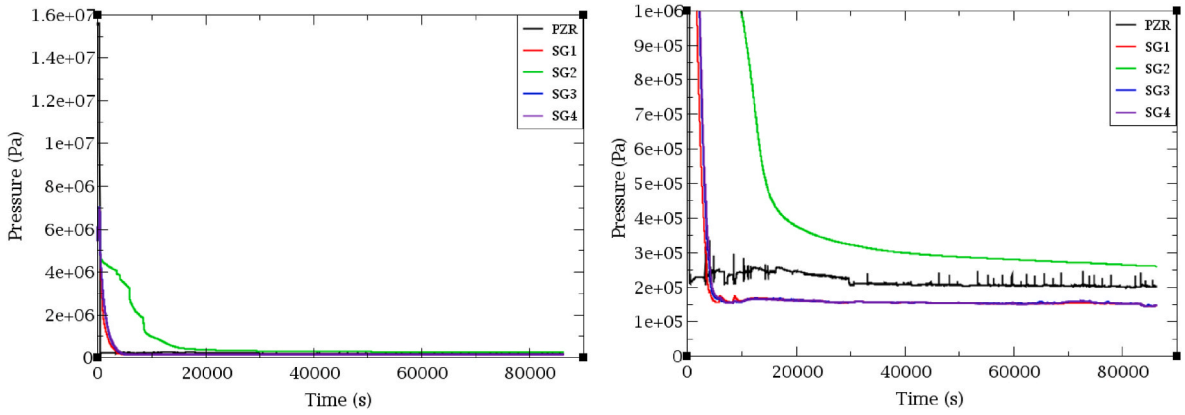

Fig. 28. RCS and SGs pressure (left) and RCS and SGs pressure (y-axis zoomed in) (right); DEGB LBLOCA along with SBO sequence.

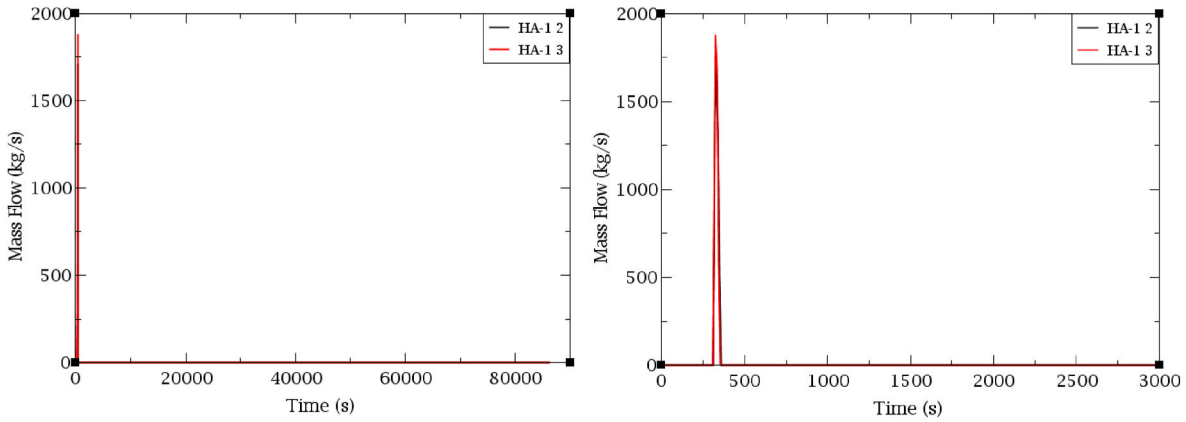

Fig. 29. HA-1 mass flow rate (left) and HA-1 mass flow rate (x-axis zoomed in) (right); DEGB LBLOCA along with SBO sequence.

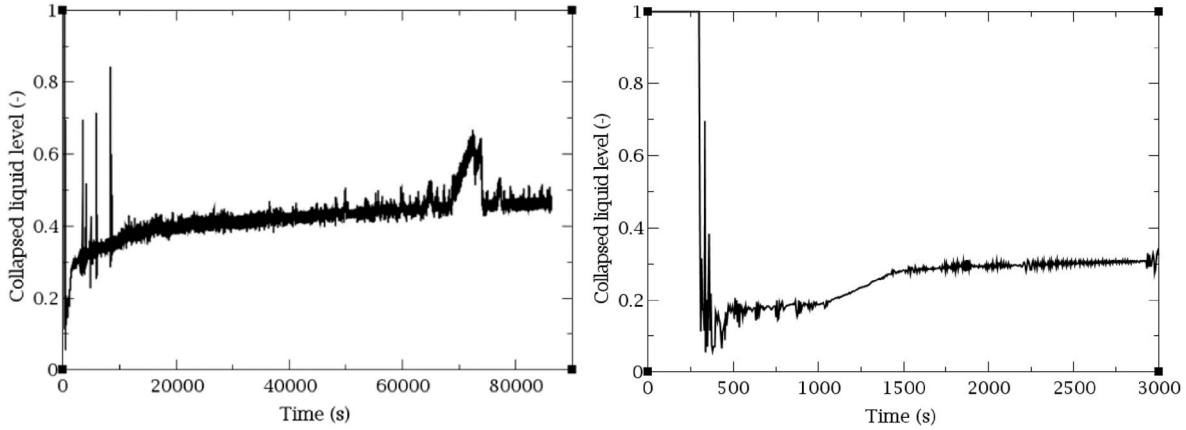

Fig. 30. Core collapsed liquid level (left) and core collapsed liquid level (x-axis zoomed in) (right); DEGB LBLOCA along with SBO sequence.

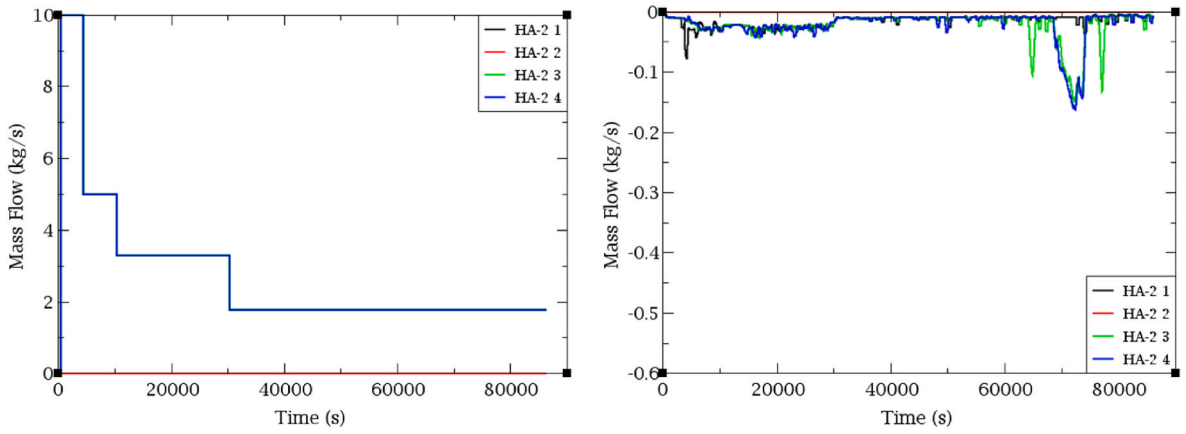

Fig. 31. HA-2 mass flow rate (left) and HA-2-CLs line mass flow rate (right); DEGB LBLOCA along with SBO sequence.

available literature was consulted and only one reference was found where the containment pressure in a LOCA due to a PZR surge line break under SBO conditions (no containment sprays available) stabilized at around 0.14 MPa, (ROSATOM, 2022). Therefore, in the present analysis for a significantly smaller break, the selected boundary condition for the containment pressure was 0.1 MPa. Subsequently, to verify the impact of a higher pressure on the containment, a second case was simulated with a containment pressure of 0.2 MPa, finding that the impact of this difference was negligible.

The SBLOCA break diameter is 2 inches and it is located in the CL1. The external atmospheric temperature chosen for this analysis is 303.15 K (30 °C). In addition, the SC considered for the PSS involved in the SBLOCA sequence are as follows.

- HA-1: 2 out of 4 trains
- HA-2: 3 out of 4 trains
- Air-cooled PHRS: 3 out of 4 trains

Therefore, in Section 6.1. the SBLOCA sequence under SBO conditions is first analyzed, considering the performance of the air-cooled

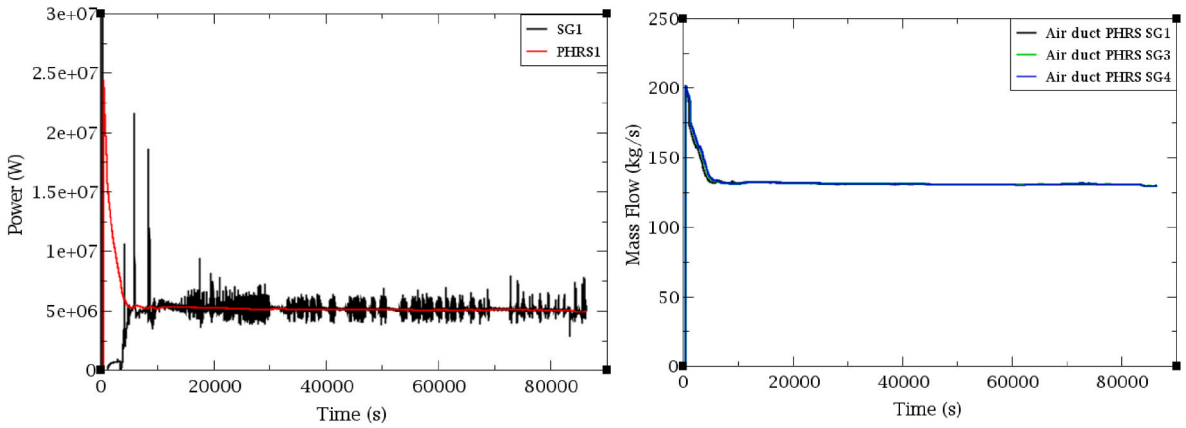

Fig. 32. PHRS 1 vs. SG 1 power (left) and PHRS air duct mass flow rate per train (right); DEGB LBLOCA along with SBO sequence.

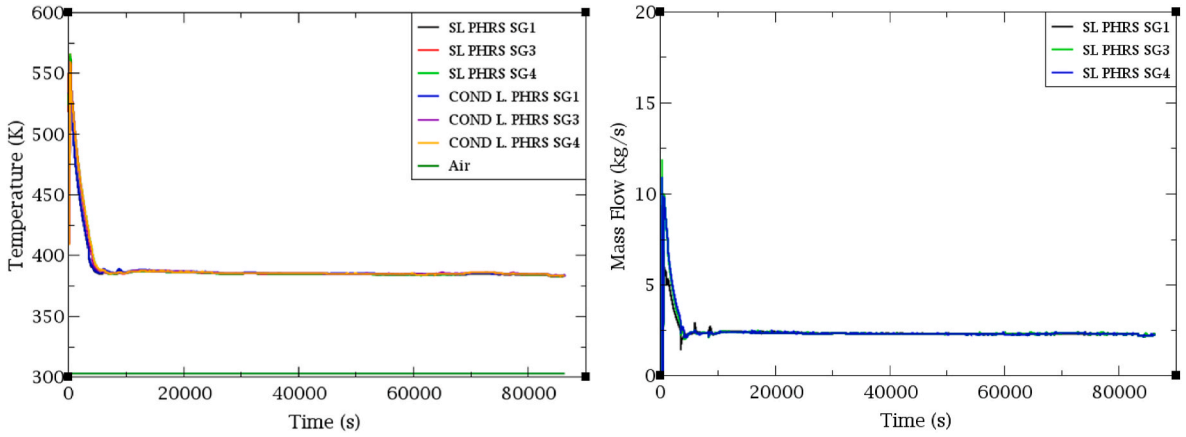

Fig. 33. PHRS steam lines and condensate lines temperature (left) and PHRS steam lines mass flow rate (right); DEGB LBLOCA along with SBO sequence.

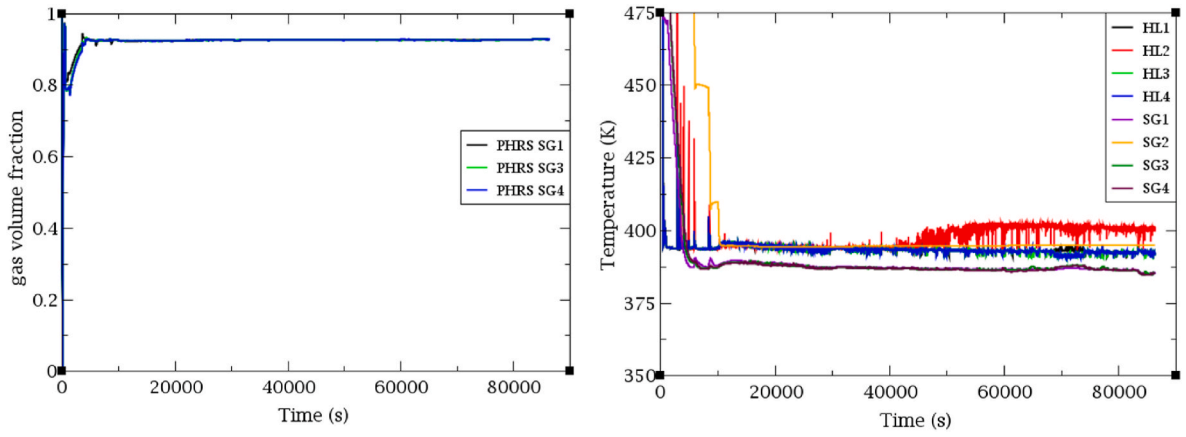

Fig. 34. PHRS outlet bundle tubes void fraction (left) and HLs and outlet SGs temperatures (right); DEGB LBLOCA along with SBO sequence.

PHRS in addition to the HA-2 PSS. Then, in Section 6.2, the SBLOCA along with SBO sequence is analyzed without considering the actuation of one PSS (HA-2 or PHRS), in order to confirm the necessity of their actuation for the success of the sequence.

6.1. SBLOCA along with SBO sequence with PHRS and HA-2 available

In this analysis, the SBLOCA is coincident with the SBO at 300 s, Fig. 16. At that instant there is a total loss of AC power, with no availability of the EDGs, which causes the SCRAM, the loss of the CVCS, RCPs trip, MFW pumps trip, TT and loss of the condenser. The evolution of the main events is shown in Table 7.

At the beginning of the transient the PHRS air gates begin to open 30 s after the SBO and they take about 90 s to fully open. Moreover, simultaneously with SBO, the SGs pressure starts to increase until it reaches the set point of the BRU-A valves at 310 s. At 485 s, the sub-cooling signal ($T_{sat} - T_{HL} < 8$ °C) occurs, causing the air-cooled PHRS to switch from the SG pressure maintenance mode to the RCS cool-down mode. The total opening of the air duct regulators causes a gradual decrease in the SGs pressure, see Fig. 17. When the pressure in the steam

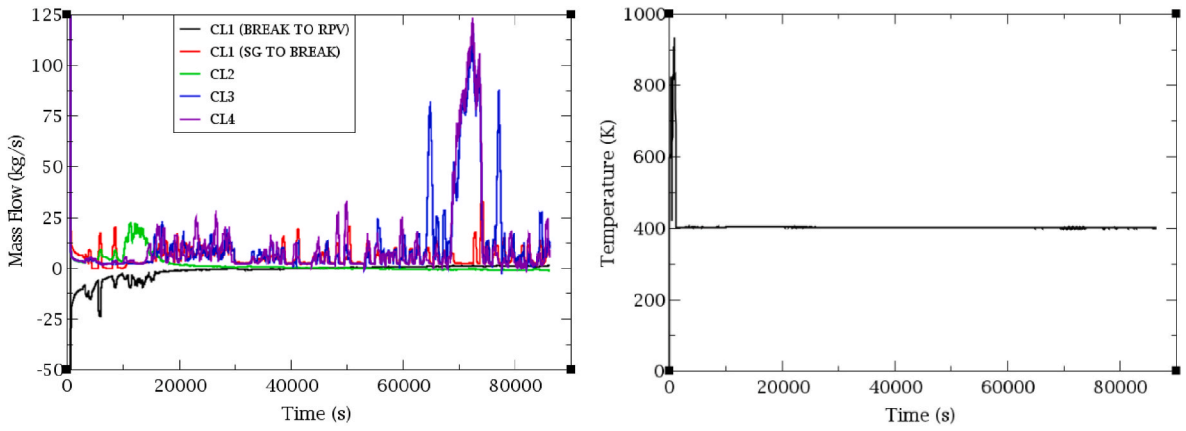

Fig. 35. RCS mass flow rate (left) and Peak Cladding Temperature (right); DEGB LBLOCA along with SBO sequence.

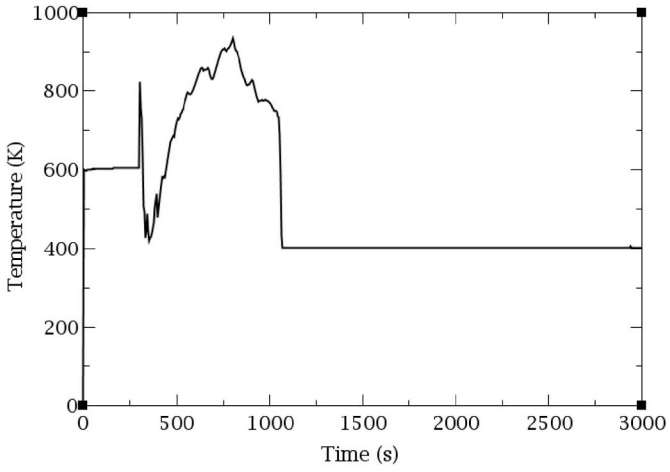

Fig. 36. Peak Cladding Temperature (x-axis zoomed in); DEGB LBLOCA along with SBO sequence.

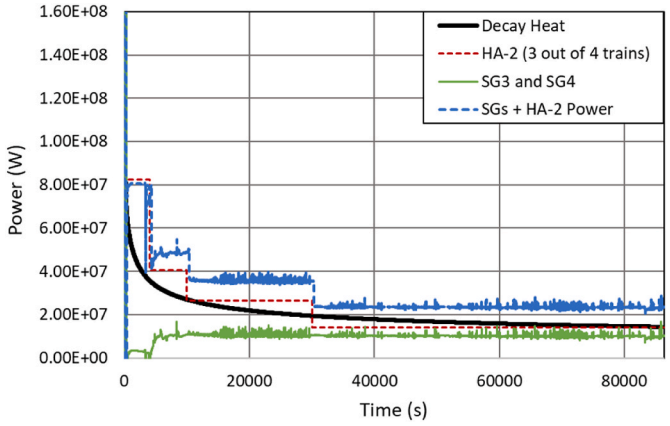

Fig. 37. Heat removal capacity of the HA-2 and PHRS vs. decay heat in the DEGB LBLOCA along with SBO sequence.

lines reaches 4.69 MPa, the MSIV isolation signal is generated.

In the RCS side, the PHRS operation allows it to cool down through the SGs, see Fig. 20 (left), resulting in an RCS pressure drop that reaches the HA-1 set-point at 2275 s. The injection of the HA-1, which empties at 7211 s, causes an increase in the core collapsed liquid level, see Fig. 18. The HA-2 pressure set-point is reached at 5640 s, but they do not start injecting until 100 s later due to a delay in the signal. The second stage of the HA-2 injection starts at 9640 s, the third stage at 15640 s and finally the fourth stage at 35640 s, see Fig. 19 (left). On the other hand, due to the emptying of the HA-2, there is inventory from the CLs sucked up by the HA-2 upstream, see Fig. 19 (right).

In the air ducts, it is observed that the air flow is about 200 kg/s per train at the beginning of the sequence and decreases to about 125 kg/s after 24 h, as shown in Fig. 20 (right). This decrease in the air flow is due to a cooling of the inventory passing through the PHRS tubes, see Fig. 21 (left). The temperature difference between the air which is at 303.15 K and the SG secondary side inventory which is in saturation at 374.15 K results in a natural circulation in the steam lines and the condensate lines of the PHRS of 1.92 kg/s after 24 h of the sequence, see Fig. 21 (right). It can also be observed that the void fraction at the outlet of the PHRS tubes is about 93 %, see Fig. 22 (left), causing a mixture of steam and saturated liquid to return to the SGs.

Moreover, in the 3 loops with PHRS available, the saturated SG inventory is at a lower pressure than the RCS, which is also in saturation conditions, so there is a temperature difference of approximately 10 K between the two, see Fig. 22 right, which leads to 25 kg/s of natural circulation induced mass flow rate in the RCS, see Fig. 23 left. It can be noted that there is no natural circulation in the loop 2 because the PHRS is not available. Finally, no CD occurs during the first 24 h of the SBLOCA along with SBO sequence, see Fig. 23 (right).

During LOCA sequences, two important safety functions have to be fulfilled, the decay heat removal and the RCS coolant supply. In this analysis, the performance of the PHRS together with that of the HA-2 has been verified to provide both critical safety functions. On the one hand, the PHRS removes the residual heat from the RCS and simultaneously cools and depressurizes it. On the other hand, the HA-2 ensures the replenishment of the inventory lost through the break, which also involves a certain power removal capacity.

This can be seen as the combined power removed by the SGs due to the PHRS performance and the HA-2, exceeds the core decay heat for most of the transient duration except for a time period around 5000, see Fig. 24 (blue line). However, simulations have shown that the RCS has enough inventory that the PCT is not affected.

The power that the HA-2 PSS can dissipate has been obtained by assuming that the mass flow rate (G) from the HA-2 tanks which enters the RCS at ambient temperature is completely evaporated, in a form similar to that calculated in (Elena Redondo-Valero et al., 2023).

$$Q_{vap} = G\,(h_{out} - h_{in}) = G\left(h^{sat}_{v,out} - h_{l,in}\right)$$

Identical sequences have been simulated (2 inches SBLOCA along with SBO) considering that the containment remains slightly pressurized at values between 0.1 MPa and 0.2 MPa. It has been found that both the PHRS and HA-2 continue to perform their functions in a similar manner,

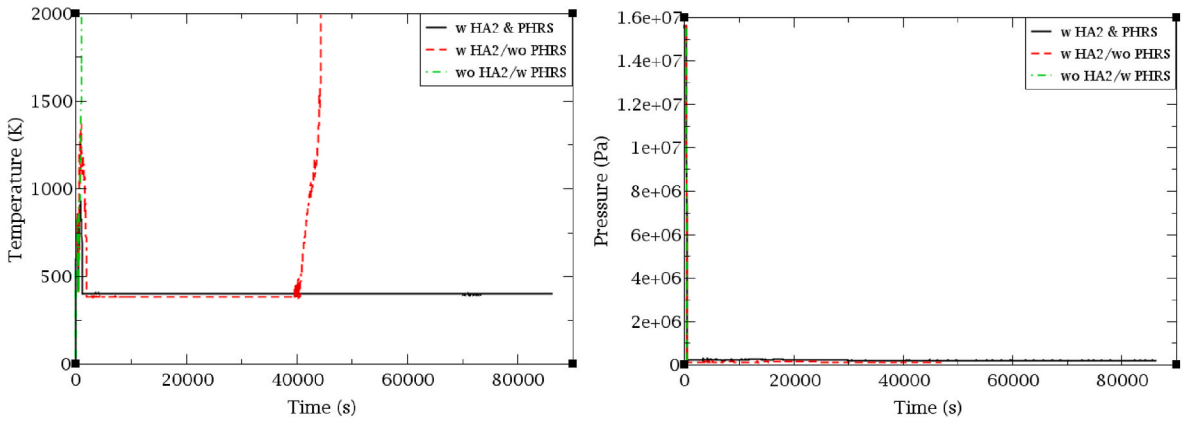

Fig. 38. PCT (left) and RCS pressure (right); DEGB LBLOCA sequence with HA-2 and PHRS, with HA-2 and without PHRS, without PHRS and with HA-2.

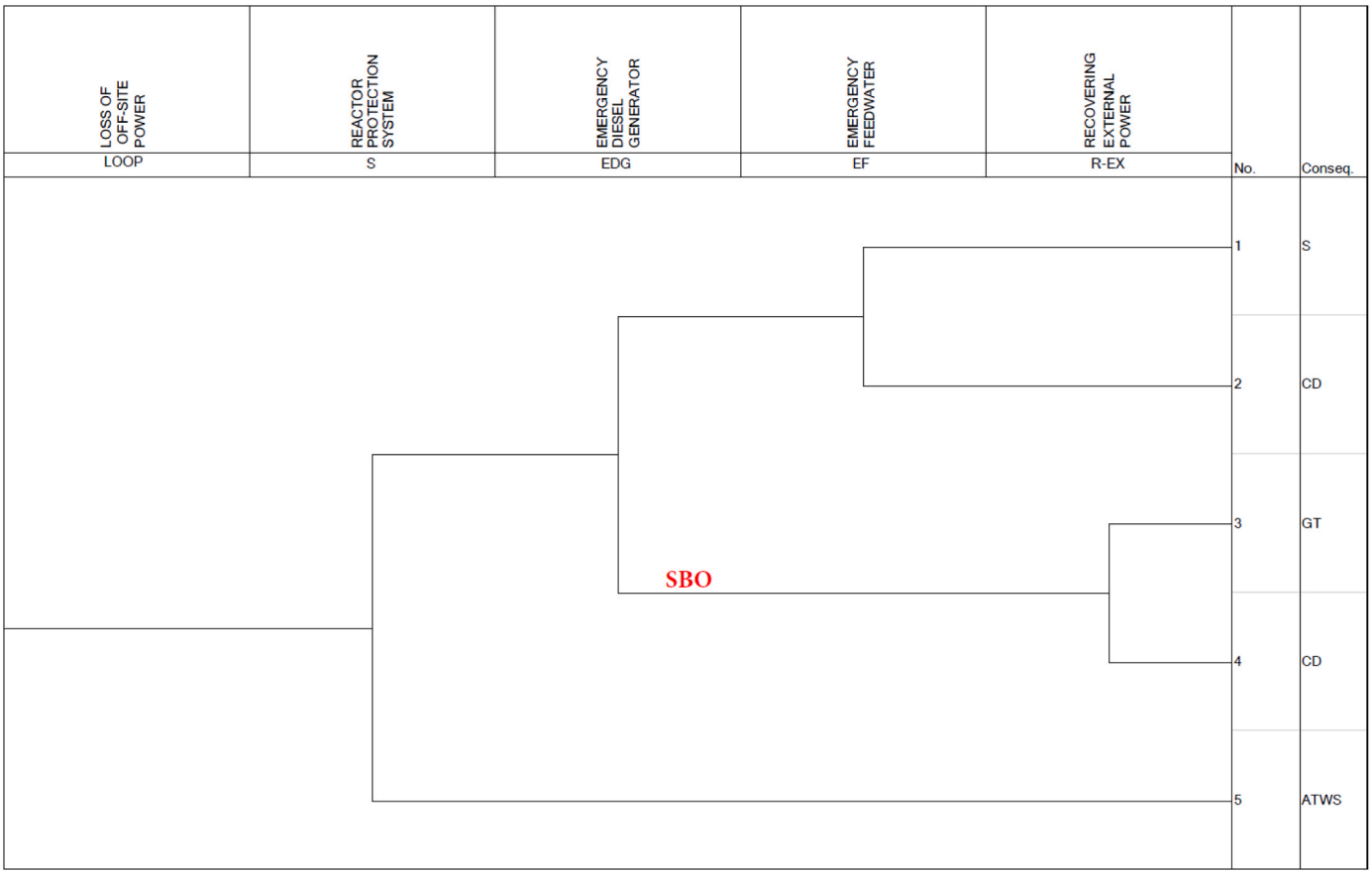

Fig. 39. Standard loop event Tree for VVERN-1000/V320.

ensuring that core uncovering does not occur and therefore the PCT does increases over 24 h.

6.2. SBLOCA along with SBO sequence; without PHRS or HA-2 availability

The aim of this subsection is to find out how the SBLOCA sequence evolves without the performance of the PSSs in order to determine whether any safety critical functions are not fulfilled. Therefore, both cases are studied, the sequence without consider the PHRS actuation and the sequence without consider the HA-2 actuation.

If only the HA-2 is available and not the PHRS, the CD occurs at about 5000 s, see Fig. 25 (left). This is because the PHRS is needed to cool the RCS and thus depressurize it to reach the HA-2 pressure set-point, see Fig. 25 (right). Therefore, no PSSs are fulfilling the heat removal and the RCS coolant replenishment critical safety function. This was found in a previous analysis, see (Elena Redondo-Valero et al., 2023).

When considering the availability of the PHRS and not the HA-2, the CD also occurs. The reason for this is that although the PHRS is able to remove much of the decay heat, there is no PSS to replenish the RCS inventory, so that the core uncovering takes place at around 40000 s, see Fig. 25 (left).

In summary, it has been shown that for the SBLOCA sequence with SBO to be successful, it is necessary for the HA-2 and the PHRS to operate together, since if they perform separately, the two safety-critical functions in this sequence are not fully achieved.

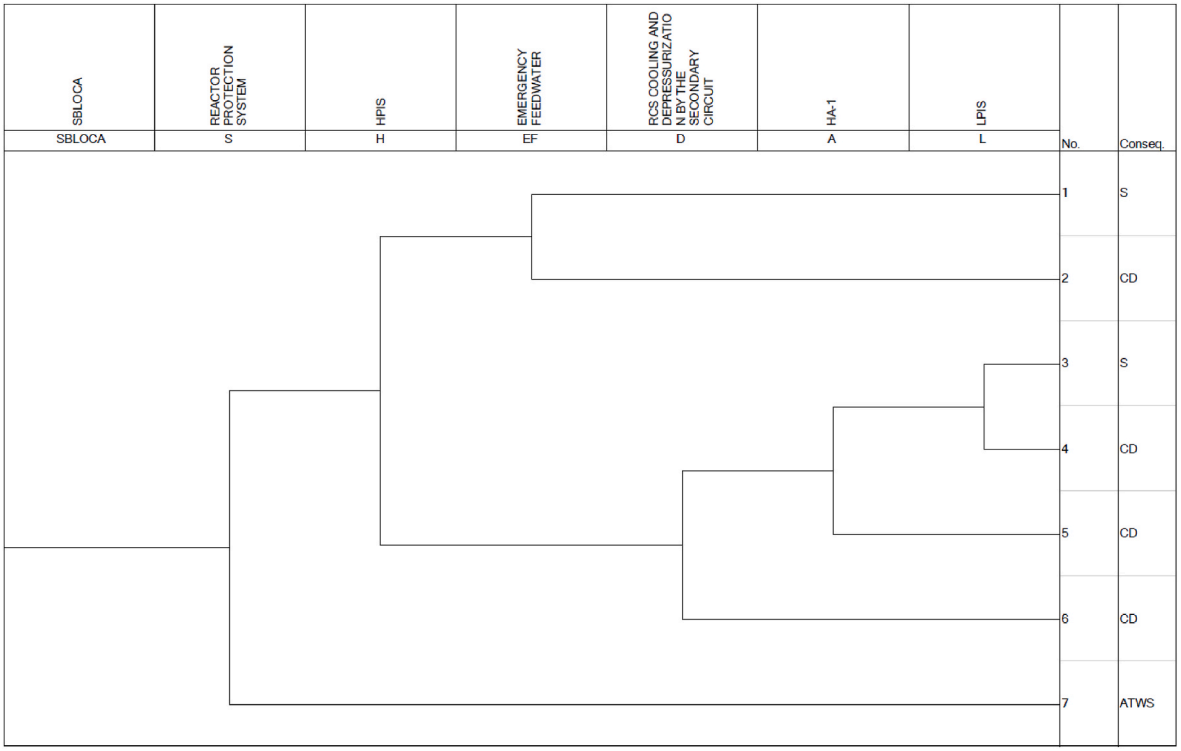

Fig. 40. Standard SBLOCA event Tree for VVER-1000/V320.

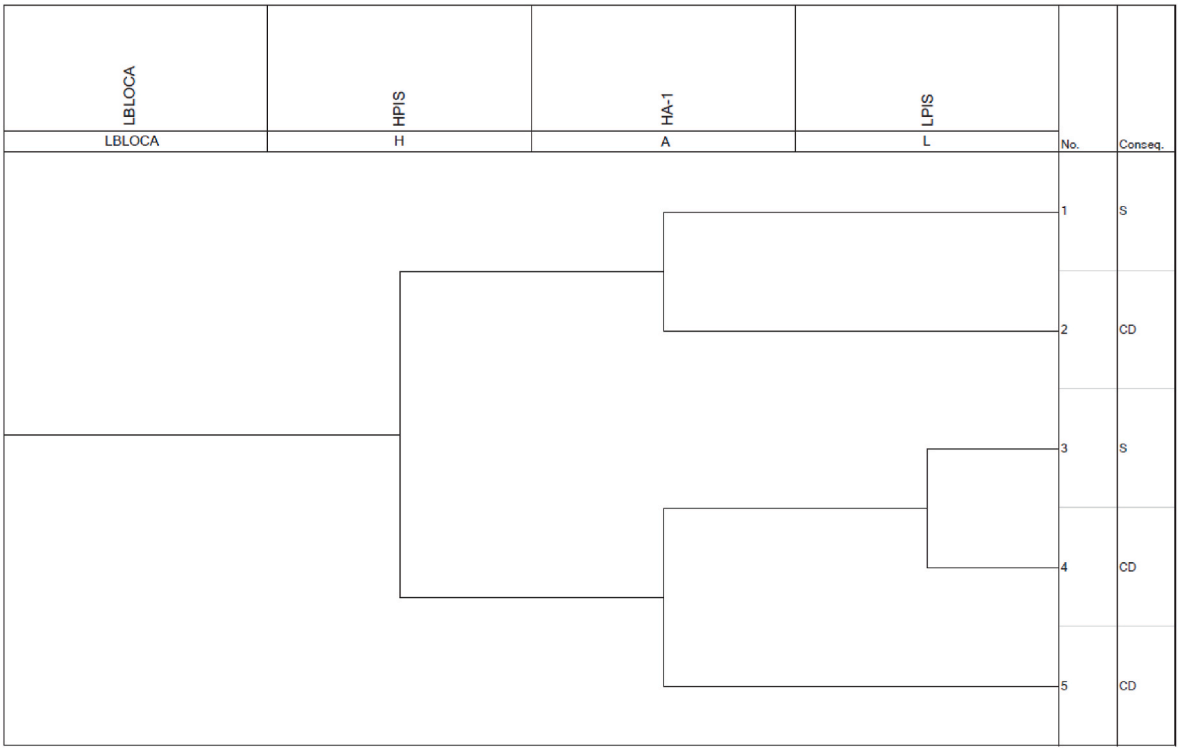

Fig. 41. Standard LBLOCA event Tree for VVER-1000/V320.

7. Performance of the PHRS and HA-2 in LBLOCA along with SBO sequences

The aim of this section is to determine the performance of the PHRS in RCS cool-down mode in a Double Ended Guillotine Break (DEGB) LBLOCA sequence under SBO conditions. It is noteworthy that there is a high interest in this sequence, as it has been analyzed in (IAEA, 2012; ROSATOM, 2022) for Gen III/Gen III + VVER designs.

In order to determine the containment pressure in this sequence, the available literature was consulted and was found that the containment

Table 9
Headers for the LB/SBLOCA ET including the HA-2 and the PHRS.

Header	Action or safety system related with
S	
EDG	Emergency Diesel Generators
H	HPIS
EF	EFW along with the BRU-A in SG pressure maintenance mode (LOOP) EFW or AFW along with the BRU-A in SG pressure maintenance mode (SBLOCA)
D	EFW or AFW along with the BRU-A in RCS cool-down mode
PHRS	PHRS in SGs pressure maintenance mode (LOOP) PHRS in RCS cool-down mode (SBLOCA and LBLOCA)
A	HA-1
L	LPIS
HA-2	HA-2
R-EX	Recovery external power

Table 10
Success criteria for the LB/SBLOCA ET including the HA-2 and the PHRS.

Header	LOOP ET	SBLOCA ET	LBLOCA ET
S	Actuation of the reactor protection system		–
EDG	1 out of 3 EDG	–	–
H	–	1 out of 3 trains	2 out of 3 trains
EF	1 out of 3 EFW pumps + 1 out of 4 BRU-A valves (SG pressure maintenance mode)	1 out of 3 EFW pumps or 1 out of 2 AFW pumps + opening of 1 out of 4 BRU-A valves (SG pressure maintenance mode)	–
D	–	1 out of 3 EFW pumps or 1 out of 2 AFW pumps + opening and regulation of 1 out of 4 BRU-A valves (RCS cool-down mode)	–
PHRS	3 out of 4 trains (SGs pressure maintenance mode)	3 out of 4 trains (RCS cool-down mode)	3 out of 4 trains (RCS cool-down mode)
A	–	2 out of 4 trains	2 out of 4 trains
L	–	1 out of 3 trains	1 out of 3 trains
HA-2	–	3 out of 4 trains	3 out of 4 trains
R-EX	Recovery of 1 safety bus	–	–

in a LBLOCA remains pressurized in the long term, with values between 0.15 and 0.25 MPa (Lebezov et al., 2024; ROSATOM, 2022), due to the large RCS inventory discharged through the break. Therefore, in the present analysis, the containment is considered to be pressurized at 0.2 MPa.

The LBLOCA chosen corresponds to a DEGB, with an equivalent break diameter of 47 inches, located in the CL1. The atmospheric temperature chosen for this analysis is 303.15 K (30 °C). In addition, the success criteria considered for the PSS involved in the LBLOCA sequence are those of the design criteria.

- HA-1: 2 out of 4 trains
- HA-2: 3 out of 4 trains
- PHRS: 3 out of 4 trains

To this end, this sequence is first analyzed in Section 7.1. considering the performance of the air-cooled PHRS in addition to the HA-2. In the subsequent section (Section 7.2), the analysis is conducted without taking into account the actuation of the PSSs.

7.1. LBLOCA along with SBO sequence with PHRS and HA-2 available

The LBLOCA starts 300 s from the beginning of the simulation, see Figs. 26 and 27. At that instant there is a total loss of AC power, without starting the EDGs, which causes SCRAM, RCPs trip, loss of the CVCS, MFW pumps trip, TT and loss of the condenser. The evolution of events is shown in Table 8.

Due to the large size of the break, the RCS depressurizes rapidly and reaches atmospheric pressure within a few seconds, Fig. 28. The HA-1 therefore injects within 15 s of the beginning of the sequence, see Fig. 29, and the HA-2 set point is reached 10 s later, which causes the increase in the core collapsed liquid level, see Fig. 30. The second stage of the HA-2 injection starts at 4325 s, the third stage at 10325 s and finally the fourth stage at 30325 s, see Fig. 31 (left). On the other hand, due to the emptying of the HA-2, there is a small inventory from the CLs sucked up by the HA-2 upstream, see Fig. 31 (right).

The air-cooled PHRS actuation is generated by the SBO conditions. Although the air gates take 30 s to open, the SG pressure drops from the beginning of the sequence because the RCS cools the SGs by its abrupt pressure decrease. The subcooling signal ($T_{sat} - T_{HL} < 8$ °C) is reached within 5 s, which means that the air duct dampers do not close at any time during the sequence. The signal for the MSIV closure occurs at 495 s. Subsequently, as a result of the PHRS performance, the SGs pressure drops below the RCS pressure at 3500 s. From this moment, the SGs start to cool-down the RCS see Fig. 32 (left).

In the air ducts, it is observed that the air flow is about 200 kg/s per train at the beginning of the sequence and decreases to about 125 kg/s after 24 h, as shown in Fig. 32 (right). This decrease in the air flow is due to a cooling of the inventory passing through the PHRS tubes, Fig. 33 (left). The temperature difference between the air which is at 303.15 K and the SG inventory which is in saturation results in a natural circulation in the PHRS steam lines of about 2.26 kg/s after 24 h of the sequence, see Fig. 33 (right). It can also be observed that a void fraction of 92.8 % at the outlet of the PHRS tubes, see Fig. 34 (left), causing a mixture of steam and saturated liquid to return to the SGs.

Besides, the saturated SG inventory is at a lower pressure than the RCS, which is also in saturation conditions, so there is a temperature difference between the two, see Fig. 34 (right), which leads to a slight natural circulation in the 3 RCS loops with the PHRS available, see Fig. 35 (left).

As shown in Fig. 27, at approximately 700 s, the mass flow rate due to the break becomes less than the injected mass-flow rate from the three HA-2 trains available. From this point the second peak of the PCT begins to decrease, without reaching 1477 K, which marks the start of the reflooding phase. Finally, it can be concluded that no CD occurs during the first 24 h of the LBLOCA along with SBO sequence, see Fig. 35 (right) and Fig. 36.

The need to fulfil two critical safety functions in LOCA sequences has already been mentioned: decay heat removal and RCS coolant supply. As in the SBLOCA sequence, it has been verified that in the LBLOCA sequence with SBO conditions, the combined performance of the HA-2 and the PHRS ensures both critical safety functions for at least 24 h. The joined power removed by the SG3 and SG4 (SG1 is not considered because of the DEGB), due to the PHRS performance, and the HA-2 is shown together with the core decay heat in Fig. 37 (blue line). The power dissipation of the HA-2 PSS has been calculated as in the previous Section 6.1.

7.2. LBLOCA along with SBO sequence; without PHRS or HA-2 availability

In this section, both cases are studied, the LBLOCA with SBO sequence without considering the PHRS actuation and without considering the HA-2 actuation. The aim is to know when the CD is reached if one of the two critical safety functions, the heat removal and the RCS coolant supply, is not fulfilled.

If only 3 out of 4 HA-2 trains (HA-2 SC) are considered, and not the PHRS, it is found that the PHRS is not necessary for the HA-2 to start injecting water into the RCS, as the break is sufficient to allow the RCS pressure to reaches atmospheric values in a few minutes, see Fig. 38 (right). During the first three stages of HA-2 injection, the heat removed by this PSS is greater than the core decay heat, see Fig. 37 (red line), but

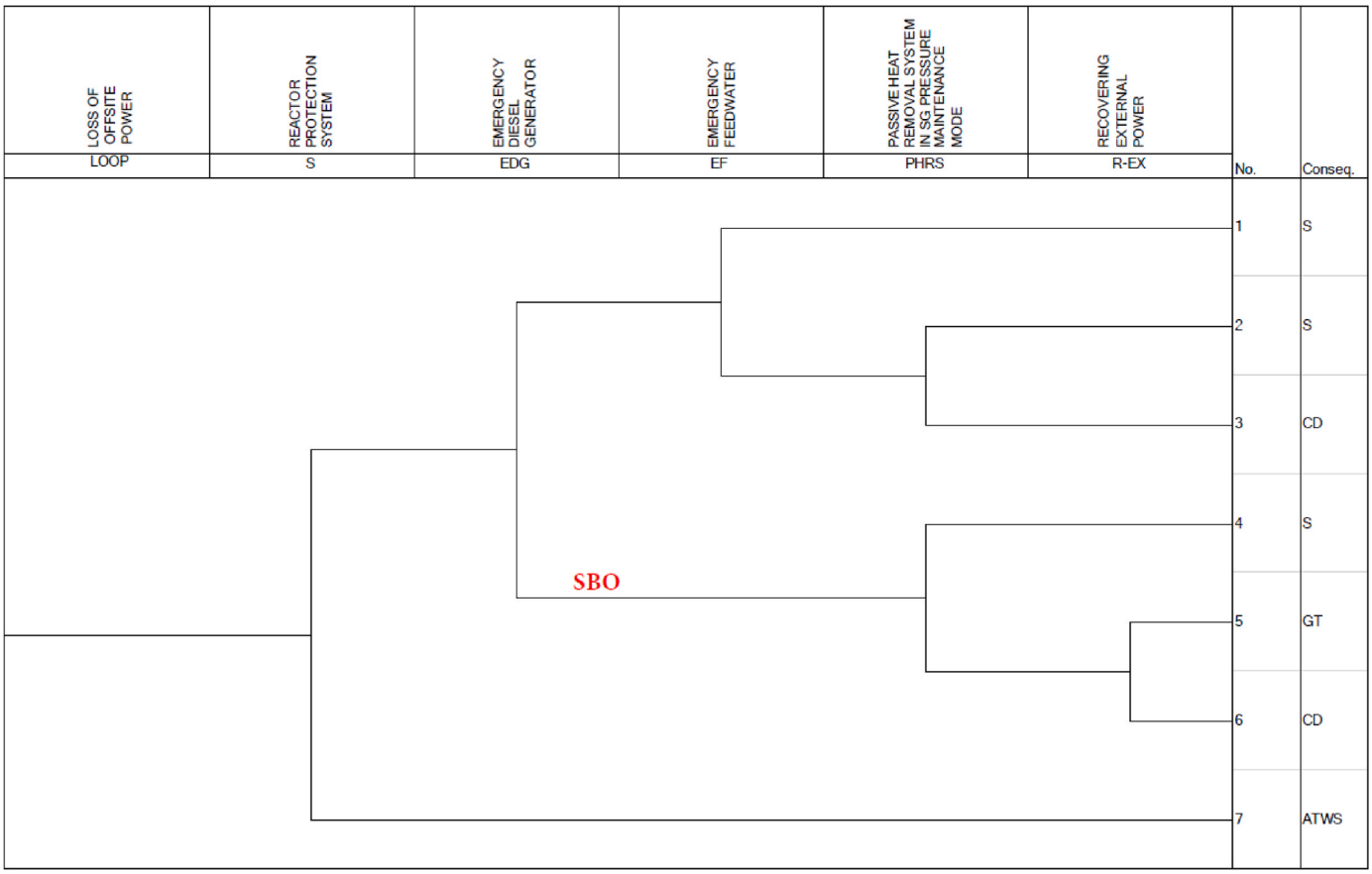

Fig. 42. Loop event Tree including the PHRS

in the fourth stage of injection, the thermal power of the core becomes greater. The result is that from 40000 s onward, the core is uncovered and subsequently the CD is reached, see Fig. 38 (left). This was found in a previous analysis, where it was also obtained that if 4 out of 4 HA-2 trains are considered instead of the success criteria number of trains, the HA-2 removal power is enough to avoid the CD during 24 h, see (Elena Redondo-Valero et al., 2023).

On the other hand, if only 3 out of 4 trains (PHRS SC) of the PHRS are available, CD is reached within a few seconds after the beginning of the accidental sequence, see Fig. 38 (left), since the inventory of the HA-1 is not sufficient to prevent the core uncovering. To conclude, it has been shown that for the LBLOCA sequence under SBO conditions the combined actuation of the HA-2 and the PHRS, considering the design criteria of both, is necessary to ensure core cooling for at least 24 h.

8. LOOP, SBLOCA and LBLOCA ETs including the HA-2 and the PHRS passive safety systems

The LBLOCA ET for the VVER-1000/V320 was reviewed in detail, the SC were verified, and new ETs were proposed in (E Redondo-Valero et al., 2023). Subsequently, in (Redondo-Valero et al., 2024), the SBLOCA ET was analyzed, with particular interest in the sequences where there is no High Pressure Injection System (HPIS) and the SGs have to be depressurized. On the other hand, in (Elena Redondo-Valero et al., 2023), an extensive study was performed on the influence of the HA-2 in LOCA sequences with SBO conditions, in order to determine the safety margin obtained with their performance. Finally, the present work has provided a comprehensive understanding of the PHRS effect, along with the HA-2, on SBO and LOCA sequences.

On the basis of all these analyses, the aim of this section is to determine how the ETs for the LOOP, SBLOCA and LBLOCA would be if new headers incorporating the HA-2 and the PHRS performance are introduced. Therefore, the standard ETs for the LOOP, SBLOCA and LBLOCA sequences are presented in Section 8.1, followed by the new proposed ETs in Section 8.2.

8.1. LOOP, SBLOCA and LBLOCA standard ETs

The standard LOOP ET for the VVER-1000/V320 is based on that found in (Begun et al., 2000; Science Applications International Corporation SAIC, 1987), see Fig. 39. On the other hand, the SBLOCA and the LBLOCA ETs considered, see Figs. 40 and 41, come from previous studies carried out at the UPM (E Redondo-Valero et al., 2023; Redondo-Valero et al., 2024) and are based on the ETs included in (Skalozubov et al., 2010).

The description of the headers is given in Table 9. Note that all the headers correspond to the same functions for the LOOP, SBLOCA and LBLOCA ETs, with the exception of the EF header. This header includes the operation of the EFW and the BRU-A valves in the LOOP ET, but in the SBLOCA ET it includes the operation of the EFW or the Auxiliary Feed Water (AFW) together with the BRU-A valves. The SC for each header are given in Table 10.

This is especially noteworthy that the LOOP, the SBLOCA and the LBLOCA standard ETs do not include headers with safety systems capable of removing the residual heat or replenishing the RCS inventory in the long term in the event of a total loss of AC power. In the ETs, sequences reaching a successful end state are denoted by "S", while sequences reaching core damage are denoted by "CD".

8.2. LOOP, SBLOCA and LBLOCA new proposed ETs

For the LOOP sequences to be successful, it is necessary to cool the

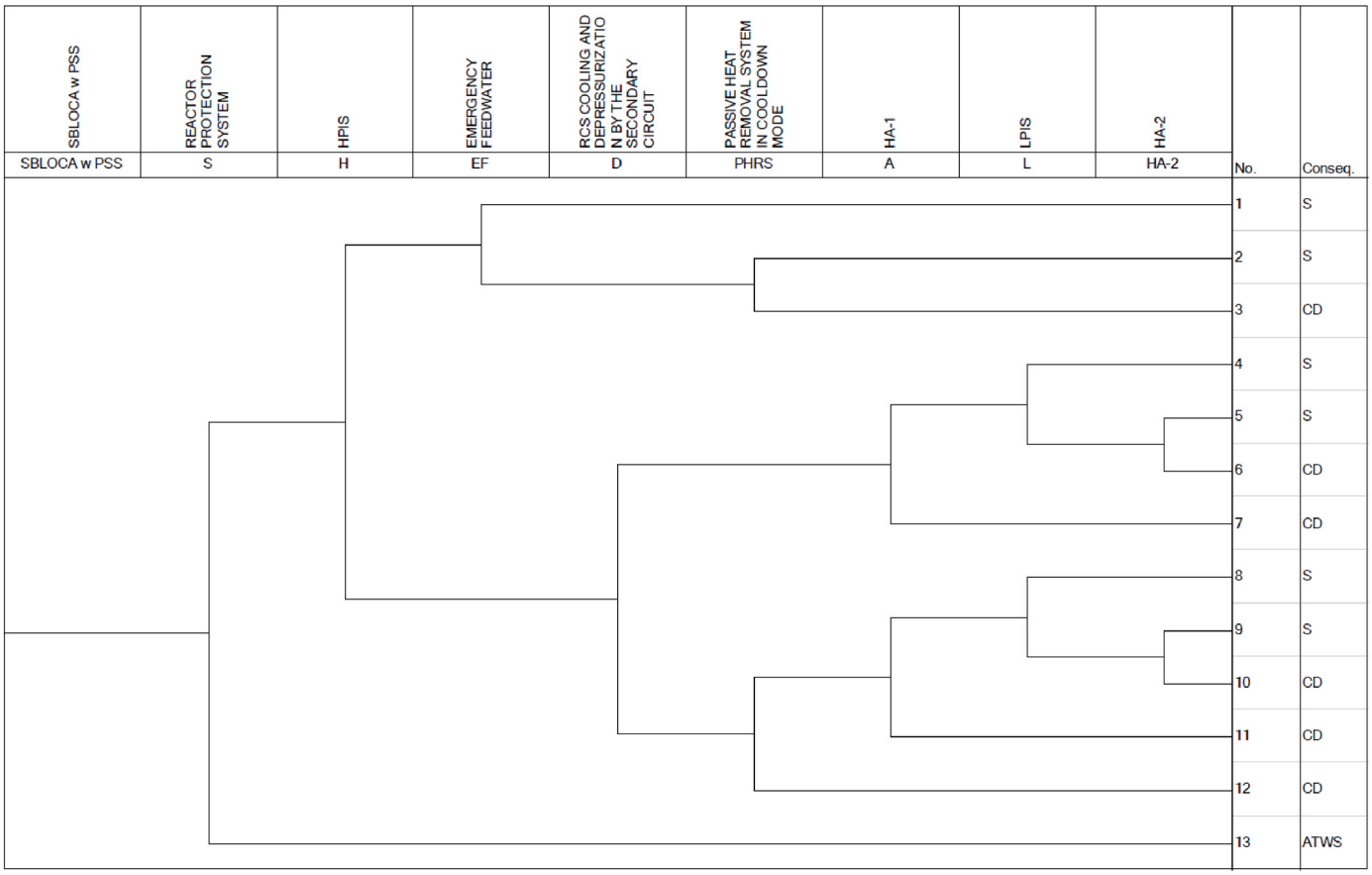

Fig. 43. Sbloca event Tree including the HA-2 and the PHRS

RCS through the SGs. This can be achieved in two ways: either by using the EDGs to start the EFW pumps, or by having the air-cooled PHRS available in SG pressure maintenance mode. If the EFW pumps or the PHRS are not available, it is imperative that the external power is restored to avoid the CD.

In SBLOCA sequences without HPIS actuation, it is necessary to cool and depressurize the RCS, in order to reach the setpoint of the low-pressure ECCS. In VVER-1000/V320 reactors, the cooling and depressurization of the RCS is achieved by the joint actuation of the EFW/AFW and the BRU-A valves, with the drawback that AC power is required. In some Gen III/III + VVERs, in a scenario where AC power is not available, this action of cooling and depressurizing the RCS is performed by the air-cooled PHRS. Once the RCS has been depressurized, the action of replenishing the inventory in the RCS is carried out by the Low Pressure Injection System (LPIS) if AC power is available. In the Gen III/III + VVER reactors with air-cooled PHRS, the low-pressure inventory replenishment action is performed by the HA-2 if the LPIS is not available.

In LBLOCA sequences, the action of cooling and depressurizing the RCS through the SGs is not necessary, even when the HPIS is not available. Therefore, the standard LBLOCA ET of the VVER-1000/V320 does not incorporate the headers corresponding to EFW (or AFW) with the BRU-A in RCS cool-down mode (D). Besides, in Gen III/III + VVER reactors with air-cooled PHRS and HA-2 PSSs, they do not require PHRS operation to depressurize the RCS and allow HA-2 operation in LBLOCA sequences without HPIS or/and LPIS unavailability. However, in the long term, the HA-2 are capable of removing decay heat for 24 h if all four trains are available, see (Elena Redondo-Valero et al., 2023). But, if 3 out of 4 trains or less are available, the power removed by the HA-2 is less than the core power, so PHRS power is required for the fourth injection stage.

Based on the above, and on the results of the simulations carried out, an ET has been defined for the LOOP, SBLOCA and LBLOCA sequences of a VVER-1000/V320 reactor incorporating the air-cooled PHRS and HA-2 PSSs, see Figs. 42–44. The headers included in the new proposed ETs are shown in Table 9, and the SC considered for the different headers can be seen in Table 10.

8.2.1. *Proposed LOOP ET*

In the LOOP ET, sequence 1 involves the successful of the S, the EDG and the EF headers. This sequence is similar to the SCRAM sequence analyzed in (Redondo-Valero et al., 2021) where it was confirmed that a successful end state is reached. In sequences 2 and 4, instead of the EF headers being successful, the PHRS header is successful, with or without the EDG header also being successful. As analyzed in section 5.1, these sequences also reach a successful end state.

On the other hand, sequences 3 and 6 lead to the CD end state, as they both involve the failure of headers related to the cooling of the SGs. In sequence 3, neither the EF nor the PHRS headers are successful. In sequence 6, both the EDG and R-EX headers fail, resulting in no EFW injection to the SGs, and the PHRS header also fails. Scenarios without EFW and PHRS were analyzed in section 5.2 and confirmed to result in a CD end state.

In contrast, sequence 5 includes the failure of the EDG, EF and PHRS headers, but with a successful R-EX header. This sequence leads to a Generic Transient (GT) sequence which is very similar to sequence 1. Finally, if the S header fails, there is an immediate transition to the ATWS ET.

Furthermore, as previously discussed in section 5, this work does not consider RCPs leakages during the SBO conditions. However, if they were to be considered, it should be noted that in sequence 4 of the LOOP ET there would be a transfer to the SBLOCA ET as the EDG heater is not

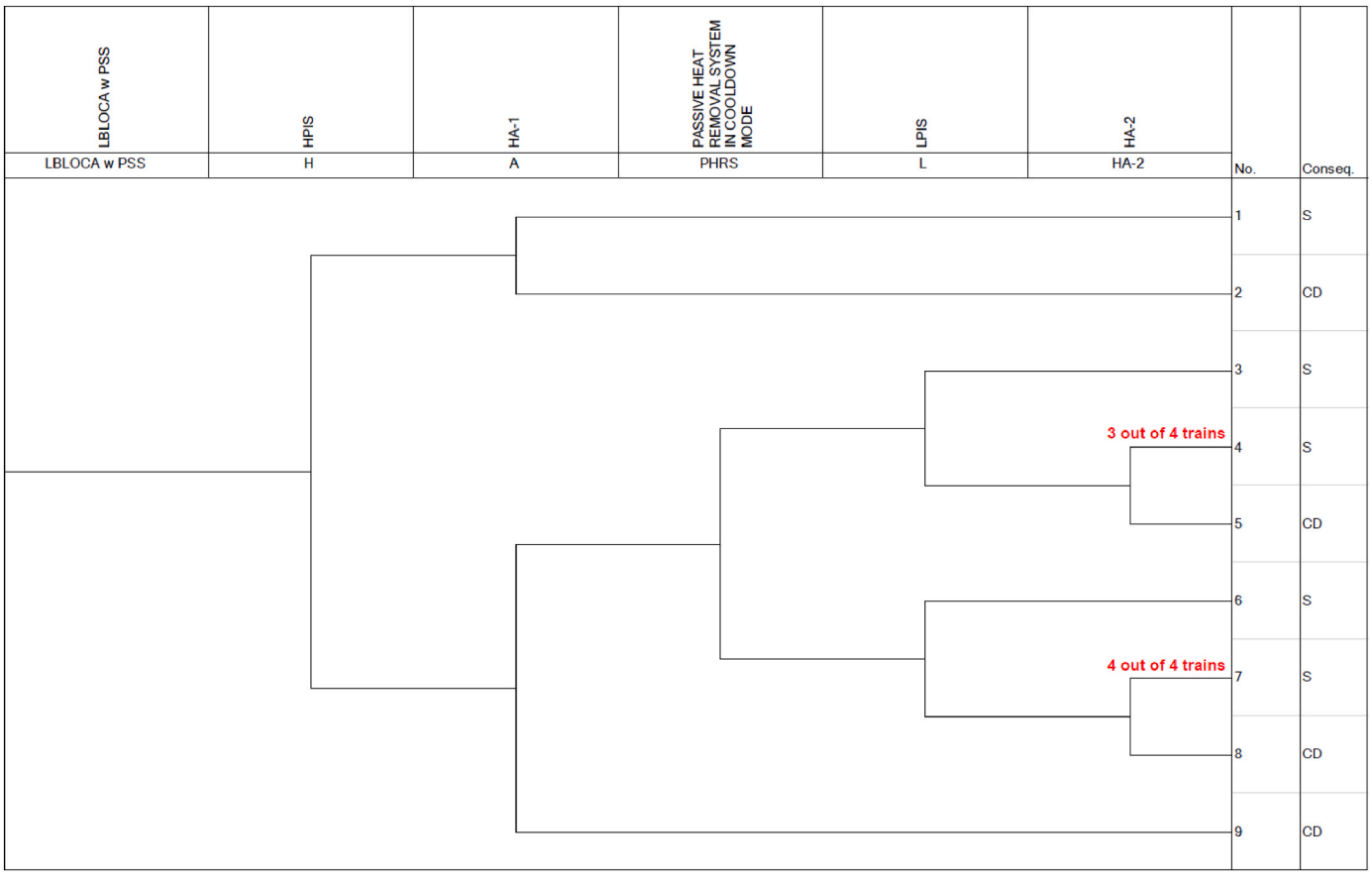

Fig. 44. Lbloca event Tree including the HA-2 and the PHRS

successful and therefore there are no CVCS pumps injecting water to the RCPs seals.

8.2.2. *Proposed SBLOCA ET*

In the SBLOCA ET, the successful end state is reached when the H header is successfully combined with either the EF header, sequence 1, or the air-cooled PHRS header, sequence 2. Sequence 1 was analyzed in (Redondo-Valero et al., 2021). Conversely, if neither the EF nor the PHRS headers are successful, CD occurs. As assumed in (Skalozubov et al., 2010), the activation of the EFW system is required for the sequence to be successful.

If the H header fails, the sequence may still succeed if either the D header or the PHRS header succeeds. In these cases, success of the A header is also required along with either the L header, sequences 4 and 8, or the HA-2 header, sequences 5 and 9. Sequence 4 was analyzed in (Redondo-Valero et al., 2024) and sequence 9 in section 6.1, both of which have been confirmed to reach a successful end state. On the other hand, sequence 12, where neither the D nor the PHRS header is successful, results in a CD end state, as has been verified in section 6.2.

It is also assumed that any sequence in which the A header fails does not lead to a successful end state, see (Skalozubov et al., 2010). Finally, in the SBLOCA ET, sequence 13 includes the failure of the S header, which results in a transition to the ATWS ET.

8.2.3. *Proposed LBLOCA ET*

In (E Redondo-Valero et al., 2023), sequence 1 of the LBLOCA ET, where both the H and A headers are successful, was analyzed and found to reach a successful end state. Conversely, in (E Redondo-Valero et al., 2023) it was also observed that the sequences where the A header fails, specifically sequences 2 and 9, do not achieve a successful end state when a 1 out of 3 SC is applied to the LPIS. In addition, this study also showed that when the only successful ECCS is the HA-1, as in sequence 8, the sequence reaches the CD end state.

The failure of the H header can still result in a success end state if the L and A headers are successful, regardless of the availability of the air-cooled PHRS, sequences 3, or not, sequence 6. It is important to note that sequence 6 was analyzed in (E Redondo-Valero et al., 2023), where it was found that the sequence did not reach the CD. Therefore, it is assumed that sequence 3, which also takes into account the availability of the air-cooled PHRS, reaches a successful end state.

Furthermore, in (Elena Redondo-Valero et al., 2023) it was found that sequence 7, where both HA-1 and HA-2 are available, can only succeed if all 4 HA-2 trains are operational. However, in section 7.1 it has been seen that sequence 4, where the PHRS is available, reaches a successful end state with a SC for HA-2 of 3 out of 4 trains. Also, the results performed in section 7.2 show that if the PHRS is available, but neither the HPIS, the LPIS nor the HA-2 are available, as in sequence 5, the CD is reached.

It is noteworthy that in the three proposed ETs with the HA-2 and the PHRS headers, there are success sequences in which only the headers corresponding to the PSSs are successful. However, for the standard ETs, the success of some headers related to the active safety systems is mandatory for the sequence to be successful.

9. Conclusions

In this study, a comprehensive literature review of the air-cooled PHRS has been carried out to determine its dimensions and operating modes. An isolated air-cooled PHRS model has then been developed for the TRACE system code, which has been validated with Kudankulam NPP data. Then, this model has been integrated into a model of a VVER-1000/V320 reactor which also incorporates the HA-2 PSS.

This has allowed a detailed analysis of the impact of the air-cooled PHRS and the HA-2 PSSs performance on SBO sequences, with and without a simultaneous LOCA. The following conclusions can be drawn from this work.

- The simulations of the SBO sequence show that the performance of the air-cooled PHRS, considering its design criteria, in SGs pressure maintenance mode, allows cooling the core for 24 h, preventing the RCS from boiling.
- The simulation of the SBLOCA sequence show that the performance of air-cooled PHRS, considering its design criteria, in RCS cool-down mode allows the RCS pressure to decrease, reaching the HA-2 set-point in time to avoid core uncovering.
- The simulation of the LBLOCA sequence show that the performance of the air-cooled PHRS, considering its design criteria, in RCS cooling mode, allows to keep the RCS cooled for 24 h, while operating the HA-2 with its design criteria.

The findings from these analyses, which include both passive safety systems (HA-2 and air-cooled PHRS) and previous analyses on the VVER-1000/V320 reactor with conventional safety systems realized by the UPM research group, have contributed to the proposal of new ETs for the SBLOCA, LBLOCA and LOOP sequences.

In summary, the results show that the safety margins are significantly increased as the alternatives to prevent core damage in the analyzed sequences are diversified, thus reducing the conditional probability of damage.

As a final conclusion, this paper makes a significant contribution to the open literature on two passive safety systems common of Generation III VVER reactors, the HA-2 and the air-cooled PHRS. It not only presents their layout and geometric parameters but also demonstrates their ability to manage SBO and LOCA along with SBO sequences without human intervention in a Generation II VVER-1000/V320 model using the TRACE system code.

CRediT authorship contribution statement

Elena Redondo-Valero: Writing – review & editing, Writing – original draft, Software, Resources, Methodology, Investigation, Formal analysis, Conceptualization. **Cesar Queral:** Writing – review & editing, Supervision, Resources, Methodology, Conceptualization. **Kevin Fernandez-Cosials:** Writing – review & editing, Resources, Methodology, Conceptualization. **Victor Hugo Sanchez-Espinoza:** Writing – review & editing, Resources, Methodology, Conceptualization.

Declaration of competing interest

The authors declare that they have no known competing financial interests or personal relationships that could have appeared to influence the work reported in this paper.

Acknowledgement

This work in the framework of the Grant PID2019-108755RB-I00 (ISASMORE) funded by MCIN/AEI/10.13039/501100011033.

Data availability

The authors do not have permission to share data.

References

Agrawal, S.K., Chauhan, A., Mishra, A., 2006. The VVERs at Kudankulam. Nucl. Eng. Des. 236, 812–835.
Ahmed Pirouzmand, R., Shahabinejad, A., 2021. Thermo-hydraulic analysis of the safety system of the passive heat recovery reactor VVER1000 with use code RELAP5. Technology and Nuclear Energy 4, 32–42 (in Arabic).
Asmolov, V.G., 2011. Passive safety in VVERs. Nucl. Eng. Int. https://www.neimagazine.com/analysis/passive-safety-in-vvers/ [WWW Document].
Ayhan, H., Sokmen, C.N., 2016a. Design and modeling of the passive residual heat removal system for VVERs. Ann. Nucl. Energy 95, 109–115.
Ayhan, H., Sokmen, C.N., 2016b. Investigation of passive residual heat removal system for VVERs: effect of finned type heat exchanger tubes. Appl. Therm. Eng. 108, 466–474.
Ayhan, H., Sokmen, C.V., 2015. Determination of geometrical and operating parameters of PRHRS for VVER reactors: cooling by natural circulation of atmospheric air. In: 24th International Conference Nuclear Energy for New Europe (NENE). Portoroz, Slovenia.
Bajorek, S., 2007. AP1000 passive safety systems. AP1000 Design Workshop. AP1000 Design Workshop.
Begun, B.V., Gorbunov, O.V., Kadenko, I.N., Pismenny, E.N., Zenyuk, A.Y., Litvinsky, L. L., 2000. Probabilistic Safety Analysis of a Nuclear Power Plant (PSA). Ministry of education and science of Ukraine.
Berkovich, V.M., Korshunov, A.S., Taranov, G.S., Kalyakin, S.G., Morozov, A.V., Remizov, O.V., 2006. Development and Validation of a technology for removal of noncondensing gases to ensure the operability of a passive heat removal system. Atom. Energy 100.
Bezlepkin, V., Semashko, S., Alekseev, S., Ivanova, M., Vardanidze, T., Petrov, Y., 2014. Improvement of the system for passive heat removal through steam generators (SG PHRS) in NPP VVER-1200 in the light of "Fukushima" accident). In: Proceedings of the 2014 22nd International Conference on Nuclear Engineering (ICONE22). Prague, Czech Republic.
Bharat Heavy Electricals Limited, n.d. Technical Conditions of Contract (TCC). Volume-ia, Part-II, Chapter-2. Technical specifications and scope of work detailed. https://bhel.com/sites/default/files/tcc_2-1605099120.pdf.
Bryk, R., Mull, T., Schmidt, H., 2019. Experimental investigation of LWR passive safety systems performance at the INKA test facility. E3S Web of Conferences. Research & development in power engineering, Research & development in power engineering 137, 01035.
Buchholz, S., Krussenberg, A., Schaffrath, A., 2015. Safety and international develpment of small modular reactors (SMR) - a study of GRS. Atw. Internationale Zeitschrift fuer Kernenergie 60, 645–653.
Burgazzi, L., 2012. Chapter 2 reliability of passive systems in nuclear power plants. In: NUCLEAR POWER – PRACTICAL ASPECTS. Wael Ahmed.
Chaudhary, S., Krishna Kumar, P., Rammohan, H.P., 2017. Study of performance of passive air cooled heat exchangers as a safety system for nuclear power plants. In: Proceedings of the 24th National and 2nd International ISHMT-ASTFE. Heat and Mass Transfer Conference (IHMTC-2017). BITS Pilani, Hyderabad, India.
Chetal, S.C., 2011. 500 MWe PFBR : Concept to Realisation and Approach for Future 500 MWe FBRs. Vienna, Austria.
China Nuclear Engineering Group Corporation (CNEC), 2019. HTR PM technology (pebble bed reactor). https://www.youtube.com/watch?v=op_Zzscs73U [WWW Document].
Choi, J.-B., 2009. Status of fast reactor and pyroprocess technology development in Korea. In: International Conference on Fast Reactors and Related Fuel Cycles (FR09). Kyoto, Japan.
De Grandis, S., Apostol, M., Saverio Nitt, F., 2019. D1: Project Presentation. Passive Isolation Condenser. PIACE Project, Passive Isolation Condenser. PIACE project.
Dolganov, K.S., 2024. Integral simulation of the first 3 weeks of severe accident at Fukushima Daiichi Unit 1 with SOCRAT code. Part I – qualification of model and simulation of the initial phase. Nucl. Eng. Des. 416.
Ekariansyah, A.S., Widodo, S., Susyadi, Tjahjono, H., 2021. Preliminary Assessment of Engineered Safety Features against Station Blackout in Selected PWR Models, vol. 23. Tri Dasa Mega, pp. 47–56.
Elkin, I.V., Melikhov, O.I., Melikhov, V.I., Nikonov, S.M., Kapustin, A.V., Selkin, S.S., 2018. Experimental studies in the PSB-VVER bench of thermal hydraulics of emergency modes at NPPs with VVER-TOI. Technologies for Supporting the Life Cycle of NPP 4 (in Russian). https://elibrary.ru/item.asp?id=36825404.
Galiev, K.F., Yaurov, S., Goncharov, V., Ye, V., Volnov, A.S., 2017. Experience of commissioning of the V-392M reactor plant passive heat removal system. Nuclear Energy and Technology 3, 291, 196.
Gluekler, EmilL., 1997. U.S. Advanced liquid metal reactor (ALMR). Prog. Nucl. Energy 31, 43–61.
Heung Chang, S., Ho Kim, S., Young Choi, J., 2013. Design of integrated passive safety system (IPSS) for ultimate passive safety of nuclear power plants. Nucl. Eng. Des. 260, 104–120.
IAEA, 2019. Passive Safety Systems in Water Cooled Reactors: an Overview and Demonstration with Basic Principle Simulators.
IAEA, 2016. Design safety considerations for water cooled. Small Modular Reactors Incorporating Lessons Learned from the Fukushima Daiichi Accident.
IAEA, 2012. Natural Circulation Phenomena and Modelling for Advanced Water Cooled Reactors. IAEA-TECDOC-1677.
IAEA, 2011. Status Report 82 - KERENATM (KERENATM).
IAEA, 2009. Passive safety systems and natural circulation in water cooled nuclear power plants. IAEA-TECDOC-1624.
IAEA, 1999. Status of liquid metal cooled fast reactor technology. IAEA-TECDOC-1083.
IAEA, 1994. Technical feasibility and reliability of passive safety systems for nuclear power plants. In: Proceedings of an Advisory Group Meeting. IAEA-TECDOC-920. Germany.
IAEA, 1991. Safety Related Terms for Advanced Nuclear Plants.
Jensen, S.E., Ølgaard, P.L., 1995. Description of the Prototype Fast Reactor at Dounreay. Riso National Laboratory. DK-4000 Roskilde, Denmark.

Kaliatka, A., 2017. Issues related to the safety assessment of the SMR concepts. In: Technical Meeting on Challenges in the Application of the Design Safety Requirements for Nuclear Power Plants to Small and Medium Sized Reactors. Vienna, Austria.

Khubchandani, P., Srivastava, A., Lele, H.G., 2013a. Reliability assessment of passive heat removal system of VVER-1000 at Kudankulam NPP. In: The 15th International Topical Meeting on Nuclear Reactor Thermal - Hydraulics. NURETH-15. Pisa, Italy.

Khubchandani, P., Srivastava, A., Lele, H.G., 2013b. Reliability assessment of the passive heat removal system of the VVER-1000 reactor at Kudankulam NPP. Kerntechnik 78, 489–495.

Kolev, N., Petrov, N., Donov, J., Angelova, D., Aniel, S., Royer, E., Nikonov, S., 2006. VVER-1000 Coolant Transient Benchmark - Phase 2 (V1000CT-2), vol. 11. MSLB Problem - Final Specifications, Phase. MSLB Problem - Final Specifications.

Kopytov, I.I., Kalyakin, S.G., Berkovich, V.M., Morozov, A.V., Remizov, O.V., 2009. Experimental investigation of non-condensable gases effect on Novovoronezh NPP-2 steam generator condensation power under the condition of passive safety systems operation. In: Proceedings of the 17th International Conference on Nuclear Engineering (ICONE17). Brussels, Belgium.

Kopytov, I.I., Maltsev, M.B., Taranov, G.S., Kalyakin, S.G., Remizov, O.V., Morozov, A.V., 2011. Experimental study of NV NPP-2 steam generator model operation in condensation mode by steady states technique. In: 19th International Conference on Nuclear Engineering (ICONE19). Chiba, Japan.

Kurisaka, K., 2012. Study on preliminary level-1 PSA for Japan sodium-cooled fast reactor. NEA/CSNI/R(2012)2. In: Workshop on PSA for New and Advanced Reactors OECD Conference Centre. Paris, France.

Lebezov, A.A., Morozov, A.V., Shlepkin, A.S., Sakhipgareev, A.R., Soshkina, A.S., 2024. Experimental study of heat and mass transfer processes affecting the duration of operation of VVER passive core cooling systems. Nuclear Engineering and Desing 419.

Ma, Y., Zhang, J., Wang, M., Tian, W., Chen, R., Wu, Y., Su, G.H., Qiu, S., 2021. Performance analysis of PRHRS in primary and secondary circuit for offshore floating nuclear plant. Ann. Nucl. Energy 164.

Martinez-Gonzalez, Y., Queral, C., Redondo-Valero, E., Sanchez-Torrijos, J., 2024. Simulation of MOTEL experimental test MS-SG01 and MS-SG02 using TRACE code. In: 7th International Conference on Nuclear and Renewable Energy Resources (NURER 2024). Antalya, Turkey.

Morozov, A.V., Remizov, O.V., Kalyakin, D.S., 2014. Experimental investigations of thermal–hydraulic processes arising during Operation of the passive safety systems used in new projects of nuclear power plants equipped with VVER reactors. ISSN 00406015, Thermal Engineering 61, 357–363.

Morozov, A.V., Sakhipgareev, A.R., 2017. Experimental estimation of the effect of contact condensation of steam–gas mixture on VVER passive safety systems operation. Nuclear Energy and Technology 3, 98–104.

NRC, 2017. TRACE V5.840 user manual: input specification. Input specification. User's Manual.

NuScale Power LCC, 2020. NuScale Standard Plant – Desing Certification Application. Revision 5.

Polunichev, V.I., Shumailov, G.P., Gorbunov, P.A., Grigor'ev, M.M., Plakseev, A.A., Taranov, G.S., 2007. Development and investigation of the regulator of the passive heat-removal system for the Kudankulam nuclear power plant (India). UDC 621.039.562. Atom. Energy 102.

Queral, C., Montero-Mayorga, J., Gonzalez-Cadelo, J., Jimenez, G., 2015. AP1000® Large-Break LOCA BEPU analysis with TRACE code. Ann. Nucl. Energy 85, 576–589.

Queral, C., Montero-Mayorga, J., Rivas-Lewicky, J., Rebollo, M.J., 2017. Verification of AP1000 low-margin PRA sequences based on best-estimated calculations. Ann. Nucl. Energy 104, 9–27.

Queral, C., Sanchez-Espinoza, V., Egelkraut, D., Fernandez-Cosials, K., Redondo-Valero, E., Garcia-Morillo, A., 2021. Safety systems of Gen-III/Gen-III+ VVER reactors. Nuclear España. Volume October 2021, 1-9. https://www.revistanuclear.es/wp-content/uploads/2021/10/Art.seguridad-reactores.pdf.

Rassame, S., Hibiki, T., Ishii, M., 2017. ESBWR passive safety system performance under loss of coolant accident. Prog. Nucl. Energy 96, 1–17.

Redondo-Valero, E., Queral, C., Fernandez-Cosials, K., Sanchez-Espinoza, V., 2023a. Analysis of MBLOCA and LBLOCA success criteria in VVER-1000/V320 reactors: new proposals for PSA Level 1. Nucl. Eng. Technol. 55, 623–639.

Redondo-Valero, Elena, Queral, C., Fernandez-Cosials, K., Sanchez-Espinoza, V., 2023b. Safety margins improvement by means of the passive second stage hydroaccumulators in a VVER-1000/V320 reactor. Nucl. Eng. Des. 414.

Redondo-Valero, E., Queral, C., Fernandez-Cosials, K., Sanchez-Espinoza, V.H., Sanchez-Perea, M., Groudev, P., 2024. Management of the SBLOCA sequences with HPIS failure in VVER-1000/V320 reactors; comparison with Westinghouse PWR strategies. Prog. Nucl. Energy 177.

Redondo-Valero, E., Queral, C., Sanchez-Espinoza, V., 2021. Thermal-hydraulic analysis of a VVER-1000/V320 reactor with TRACE5p5 code. In: Proceedings of the European Nuclear Young Generation Forum. ENYGF21. Tarragona, Spain.

Redondo-Valero, E., Sánchez-Torrijos, J., Queral, C., Cabellos, O., 2022. Analysis of a main steam line break accident in the NuScale reactor by means of the coupled codes TRACE and PARCS. In: International Youth Nuclear Congress (IYNC2022). Koriyama, Japan.

ROSATOM, 2023. Eight heat exchangers of passive heat removal system have been installed at Rooppur NPP Unit 1 [WWW Document]. https://www.rosatom.ru/en/press-centre/news/eight-heat-exchangers-of-passive-heat-removal-system-have-been-installed-at-rooppur-npp-unit-1/#:~:text=PHRS%20is%20a%20passive%20safety,of%20all%20power%20supply%20sources.

ROSATOM, 2022. Course on Technological Aspects of AES-2006 (VVER-1200) Development of Nuclear Curricula on VVER Technology.

Sanchez-Espinoza, V., Bottcher, M., 2006. Investigations of the VVER-1000 coolant transient benchmark phase with the coupled system code RELAP5/PARCS. Progress in Nuclear Energy. Prog. Nucl. Energy 48, 865–879.

Sanchez-Espinoza, V., Gabriel, S., Suikkanen, H., Telkkä, J., Valtavirta, V., Bencik, M., Lestani, H., 2021. The H2020 McSAFER project: main goals, technical work program, and status. Energies 14, 6348.

Science Applications International Corporation (SAIC). Definition of baseline VVER-1000. V320 systems and evaluation of plant response to postulated accidents. https://www.researchgate.net/publication/283569468_Definition_of_Baseline_VVER-1000_V320_Systems_and_Evaluation_of_Plant_Response_to_Postulated_Accidents.

Shlepkin, A.S., Morozov, A.V., Sakhipgareev, A.R., 2020a. Experimental study of heat transfer processes during the operation of WWER steam generator in emergency mode on a single-tube model. J. Phys.: Conference Series. XXXVI Siberian Thermophysical Seminar 1677, 1–6 (STS 36) 012119.

Shlepkin, A.S., Sakhipgareev, A.R., Morozov, A.V., 2020b. Analysis of the influence of heat and mass transfer processes in the WWER equipment on the duration of effective operation of passive safety systems. J. Phys.: Conference Series. XXXVI Siberian Thermophysical Seminar 1677, 1–5 (STS 36) 012118.

Skalozubov, B., Klyuchnikov, A., Kolykhanov, B., 2010. Fundamentals of management of design accidents with loss of coolant at the power plant. National Academy of Sciences of Ukraine, Institute of NPP Safety Problems. - Chernobyl (Kiev Region): Institute of NPP Safety Issues, 2010 (in Russian).

Sri Krishna College of Engineering and Technology (SKCET), 2019. KKNN 1.3.4 field projects report. Kudankulam Nuclear Power Plant.

Surip, W., Putra, N., Antariksawan, A.R., 2022. Design of passive residual heat removal systems and application of two-phase thermosyphons: a review. Prog. Nucl. Energy 154, 104473.

Turkish Atomic Energy Authority, 2018. European "Stress test" for nuclear power plants. National Report of Turkey. Revision 2, National Report of Turkey. Revision.

Xing, J., Song, D., Wu, Y., 2016. HPR1000: advanced pressurized water reactor with active and passive safety. Engineering 2, 79–87.

Yücehan-Kutlu, O., 2019. Analysis of VVER-1200 Passive Heat Removal Systems: Steam Generator PHRS and Containment PHRS. Lappeenranta University of Technology (LUT). Master's Thesis.